

1                   **KERNEL MATRIX APPROXIMATIONS BY SUMS OF**  
2                   **EXPONENTIALS AND STABILITY OF FAST STRUCTURED**  
3                   **TRANSFORMS\***

4                   CHENYANG CAO<sup>†</sup> AND JIANLIN XIA\*

5                   **Abstract.** Sum-of-exponentials (SoE) expansions provide an efficient strategy to perform some  
6 matrix transforms. In this paper, we show that they can also serve as a valuable way to com-  
7 pute structured approximations to some kernel matrices. We first illustrate that some existing fast  
8 transforms (Hilbert, Gauss, etc.) are essentially using generalized sequentially semiseparable (SSS)  
9 structures for which the stability has been in question before. We then give comprehensive analysis of  
10 the stability of transforms via general SSS structures and rigorously prove that such transforms may  
11 have numerical errors growing exponentially, while the use of SoE expansions leads to polynomial  
12 error growth. Moreover, we give a way to further reduce the error growth to poly-logarithmic via the  
13 use of hierarchical tree structures. Our analysis reveals the two key components that ensure stabil-  
14 ity of rank-structured transforms and other algorithms: algorithm architecture and norm bounds of  
15 the generators of the structure. It concretely confirms some long-standing speculations: sequential  
16 structured matrix (like SSS) algorithms are potentially unstable, even if relevant generators have  
17 bounded norms; hierarchical structured algorithms are stable as long as relevant generator norms are  
18 bounded. SoE expansion is then just an effective way to further control the norms of the generators.

19                   **Key words.** kernel matrix, fast transform, sum-of-exponentials expansion, low-rank approxi-  
20 mation, rank-structured matrix, backward stability

21                   **AMS subject classifications.** 15A23, 15B05, 65D15, 65F55

22                   **1. Introduction.** Kernel matrices are frequently used in numerical computa-  
23 tions and data analysis. Consider a kernel matrix of the form of

24 (1.1)                   
$$H = (\kappa(x_i, y_j))_{x_i \in \mathbf{x}, y_j \in \mathbf{y}},$$

25 where  $\kappa(x, y)$  is a kernel function and  $x_i$  and  $y_j$  are points in data sets  $\mathbf{x}$  and  $\mathbf{y}$ ,  
26 respectively. The numbers of points in  $\mathbf{x}$  and  $\mathbf{y}$  may be different, but we suppose  
27  $|\mathbf{x}| = |\mathbf{y}| = n$  for convenience.

28                   We are particularly interested in some kernel matrices arising from certain trans-  
29 forms (such as Hilbert, Gauss, and Hankel transforms). A straightforward way to  
30 perform these transforms (multiplications of  $H$  with vectors) costs  $\mathcal{O}(n^2)$ . There  
31 are fast transform algorithms that can reach nearly linear complexity. One such al-  
32 gorithm that has been very popular in the studies of integral equations is based on  
33 *sum-of-exponentials* (SoE) approximations for  $\kappa(x, y)$ . They are truncated expansions  
34 in terms of sums of exponential functions. For some kernels, SoE expansions with a  
35 small number of terms can reach high accuracy and the complexity to multiply  $H$   
36 with vectors can be reduced to  $\mathcal{O}(n)$  [13, 21, 32]. These algorithms are much simpler  
37 as compared with methods such as the fast multipole method (FMM) [14], which  
38 requires to consider local-multipole and multipole-multipole expansions for certain  
39 dense translation operators. SoE-based schemes instead use translation operators  
40 that have simple diagonal forms and also have nice norm bounds [2, 6, 12, 32]. SoE  
41 expansions are also useful for accelerating some other computations [3, 4, 5, 30].

42                   This work has two main subjects: showing how SoE expansions may be used  
43 for fast structured approximations of some kernel matrices, and further providing

---

\*Submitted for review.

**Funding:** The research of Jianlin Xia was supported in part by an NSF grant DMS-2111007.

<sup>†</sup>Department of Mathematics, Purdue University, West Lafayette, IN 47907 (cao302@purdue.edu, xiaj@purdue.edu).

44 comprehensive understanding of the stability of fast algorithms like transforms in  
45 some structured matrix forms.

46 **1.1. Background on SoE expansions for fast transforms.** To prepare for  
47 later discussions, we briefly review some background materials on how SoE expansions  
48 may be used to accelerate some transforms. Like in various previous studies [2, 6,  
49 13, 16, 20, 32], our discussions focus on point sets  $\mathbf{x}$  and  $\mathbf{y}$  in (1.1) on the real line.  
50 (Extensions to higher dimensions will also be discussed later.)

51 For various kernel functions defined on one dimensional  $\mathbf{x}$  and  $\mathbf{y}$ , the methods  
52 typically represent a kernel function  $\kappa(x, y)$  in an appropriate integral form and then  
53 approximate the integral by a quadrature rule [2, 6, 13, 21, 26, 31]. As an example,  
54 one frequently used kernel function is the Cauchy kernel  $\kappa(x, y) = \frac{1}{x-y}$  corresponding  
55 to the Hilbert transform

$$56 \quad (1.2) \quad f_i = \sum_{\substack{j=1 \\ y_j \neq x_i}}^n \frac{z_j}{x_i - y_j}, \quad i = 1, 2, \dots, n,$$

57 where  $x_i$  and  $y_j$  are points in an interval  $[a, b]$  and  $z_j$ 's are scalars. When  $s = x_i - y_j >$   
58  $0$ , an SoE expansion may be obtained based on the Laplace transform followed by an  
59 appropriate quadrature approximation:

$$60 \quad (1.3) \quad \frac{1}{s} = \int_0^\infty e^{-st} dt \approx \sum_{k=1}^p w_k e^{-st_k},$$

61 where  $p$  is the number of quadrature nodes and  $t_k$  and  $w_k$  are the quadrature nodes  
62 and weights, respectively.

63 A key step in the fast Hilbert transform is to utilize the above expansion to  
64 evaluate

$$65 \quad (1.4) \quad f_i^+ = \sum_{\substack{j=1 \\ x_i > y_j}}^\alpha \frac{z_j}{x_i - y_j},$$

66 where  $\alpha$  is an appropriately chosen index (see Section 2.1.1). According to (1.3), we  
67 have

$$68 \quad (1.5) \quad f_i^+ \approx \sum_{j=1}^\alpha \sum_{k=1}^p w_k z_j e^{-(x_i - y_j)t_k} = \sum_{k=1}^p w_k \beta_{k,\alpha} e^{-(x_i - y_\alpha)t_k} \quad \text{with}$$

$$69 \quad (1.6) \quad \beta_{k,\alpha} = \sum_{j=1}^\alpha z_j e^{-(y_\alpha - y_j)t_k}.$$

70 It can be shown that  $\beta_{k,\alpha}$  for all  $k = 1, 2, \dots, p$ ,  $\alpha = 1, 2, \dots, n$  can be precom-  
71 puted via fast updates with total cost  $\mathcal{O}(pn)$  [13, 21, 32]. Following this precomputa-  
72 tion, it costs  $\mathcal{O}(p)$  to evaluate each  $f_i^+$ . Accordingly, the total cost for evaluating  $f_i^+$   
73 for all  $i = 1, 2, \dots, n$  is  $\mathcal{O}(pn)$ . Some details will be given in Section 2.1.1.

74 **1.2. Motivations and contributions.** The aforementioned evaluation process  
75 (1.5)–(2.4) is very efficient, but is not immediately intuitive to understand. The  
76 evaluation of all  $f_i$  and the update for all  $\beta_{k,\alpha}$  are performed in iterative updates of  
77 some vectors and the numerical stability is unclear.

78 In fact, the whole transform may be assembled into a structured way to perform a  
 79 fast matrix-vector multiplication. That is, the kernel matrix  $H$  in (1.1) can be approx-  
 80 imated by a structured matrix. This leads to a matrix form of the fast transform and  
 81 suggests that SoE expansions are also useful for obtaining structured approximations  
 82 of kernel matrices. Indeed, later we can see that SoE expansions produce effective  
 83 compression of some blocks of  $H$  and further have some attractive features.

84 Thus, this work aims to give an intuitive algebraic way to reveal and extract  
 85 the underlying structure within fast transforms based on SoE expansions. Next, the  
 86 structured matrix form makes it convenient to analyze the numerical error propagation  
 87 and uncover potential stability issues in the transforms. Also, we obtain another  
 88 structured matrix transform with superior stability and reduced error growth.

89 Specifically, the main contributions of this work include the following.

- 90 1. We provide an intuitive matrix version that facilitates the understanding of  
 91 the mechanism of some fast transforms and helps to make the ideas more ac-  
 92 cessible. We show that they essentially perform matrix-vector multiplications  
 93 in terms of some rank-structured approximations to relevant kernel matrices.  
 94 The SoE framework is a strategy to organize data points into certain sepa-  
 95 rated clusters that correspond accurate low-rank off-diagonal approximations.  
 96 For the Hilbert transform above, the structured form is just a generalization  
 97 of the so-called sequentially semiseparable (SSS) matrix [8, 11], represented  
 98 by a sequence of smaller matrices called generators. With SoE expansions,  
 99 the so-called translation generators further have diagonal forms.
- 100 2. The matrix version further makes it convenient to inspect the stability and er-  
 101 ror propagation of the transforms. It has long been suspected that SSS matrix-  
 102 vector multiplications may be susceptible to stability issues and the stability of SSS matrix-vector  
 103 multiplications may be much worse than that of usual full matrix-vector mul-  
 104 tiplications [1]. However, the general stability analysis is lacking. Here, we  
 105 provide a comprehensive rigorous study of the stability of (generalized) SSS  
 106 matrix-vector multiplications and show that the backward error may poten-  
 107 tially grow exponentially with respect to the matrix size (Theorem 4.9). This  
 108 clearly reveals the stability risk.
- 109 3. To improve the stability, we convert the generalized SSS form into a general-  
 110 ized form of the hierarchically semiseparable (HSS) structure [9, 29] that has  
 111 superior stability in its operations. The error propagation of generalized HSS  
 112 matrix-vector multiplications is significantly lower than with generalized SSS  
 113 forms (Theorem 4.13). What's more, when SoE expansions are used to obtain  
 114 the generalized HSS forms, the error propagation can be further reduced.
- 115 4. The studies give comprehensive insights into the stability of structured algo-  
 116 rithms like matrix-vector multiplications. That is, there are two key compo-  
 117 nents that impact the stability: *algorithm architecture* and *norm bounds of*  
 118 *generators*. The former controls the length of the error propagation path and  
 119 the latter determines the error growth rate at each algorithm step. Hierar-  
 120 chical structured algorithms like HSS ones have lower error growth than se-  
 121 quential ones like SSS. Carefully bounded norms of generators (like from SoE  
 122 expansions) can significantly lower the error growth factor. See Theorems 4.9  
 123 and 4.13 and Corollaries 4.10 and 4.14 and some numerical validations.

124 The paper is organized as follows. Section 2 shows how some fast transforms via  
 125 SoE expansions may be formulated as matrix forms by constructing generalized SSS  
 126 approximations to the kernel matrices. Section 3 further shows how SoE expansions  
 127 may be used to produce generalized HSS approximations. The stability of transforms

128 via these two types of structures is then analyzed in Section 4, with some proofs  
 129 supplied in Appendix A. The stability results are verified by some numerical tests in  
 130 Section 5. Finally, Section 6 concludes the paper.

131 The following is a collection of commonly used notation in the paper.

- 132 • Throughout the presentation, bold lower-case letters are used for vectors and  
 133 sets of points.
- 134 • Without loss of generality, assume  $\mathbf{x}$  and  $\mathbf{y}$  in (1.1) can be partitioned as

$$135 \quad (1.7) \quad \mathbf{x} = \mathbf{x}_1 \cup \cdots \cup \mathbf{x}_N, \quad \mathbf{y} = \mathbf{y}_1 \cup \cdots \cup \mathbf{y}_N,$$

136 where each cluster  $\mathbf{x}_k$  has  $m$  points so that  $\mathbf{x}_k = (x_{(k-1)m+1}, \dots, x_{km})^T$  and  
 137  $n = Nm$ , and  $\mathbf{y}_k$  has a similar form.

- 138 •  $\text{diag}(\mathbf{v})$  denotes a diagonal matrix defined by a vector  $\mathbf{v}$ .
- 139 • For a vector  $\mathbf{v}$ , a function  $f(\mathbf{v})$  represents a vector function defined entrywise.
- 140 • For a matrix  $A$ , a function  $f(A)$  is a matrix function defined entrywise. For  
 141 example,  $\exp(A)$  represents a matrix with entries  $\exp(A_{ij})$  (instead of the  
 142 usual matrix exponential).
- 143 • For a vector  $\mathbf{v}$  and a scalar  $c$ ,  $c+\mathbf{v}$  or  $\mathbf{v}+c$  is the vector resulting from entrywise  
 144 summation by  $c$ . For a matrix  $A$ ,  $c+A$  can be similarly understood.

145 **2. Matrix version of fast transforms via SoE expansions of kernel func-**  
 146 **tions.** In this section, we present some types of fast transforms in terms of structured  
 147 matrix-vector multiplications. Selected types of kernel functions are shown as exam-  
 148 ples. For simplicity, we focus on the real line with the points  $x_i \in \mathbf{x}$  and  $y_j \in \mathbf{y}$  inside  
 149 an interval  $[a, b]$  and suppose the points in each set are ordered from the smallest to  
 150 the largest. Generalization to higher dimensions will be discussed in Section 2.3.

151 **2.1. Matrix version of the fast Hilbert transform.** The first transform we  
 152 consider is the Hilbert transform defined in (1.2). It corresponds to the Cauchy kernel  
 153  $\kappa(x, y) = \frac{1}{x-y}$ .

154 **2.1.1. Fast Hilbert transform via SoE expansions.** We first provide some  
 155 details on how to quickly perform the Hilbert transform via SoE expansions for the  
 156 Cauchy kernel. The discussions in this subsection are based on [13, 21, 32].

157 To utilize the expansion in (1.3), pick  $\delta \in (0, 1)$  so that the number of  $x_i, y_j$  points  
 158 satisfying  $|x_i - y_j| \leq \delta(b-a)$  is small. Then rewrite (1.2) as

$$159 \quad (2.1) \quad f_i = f_i^+ + f_i^- + f_i^0,$$

160 where  $f_i^+$  has the form in (1.4) and consists of all  $x_i, y_j$  points satisfying  $x_i - y_j >$   
 161  $\delta(b-a)$ ,  $f_i^-$  consist of all  $x_i, y_j$  points satisfying  $x_i - y_j < -\delta(b-a)$ , and  $f_i^0$  corresponds  
 162 to the remaining points. It is then sufficient to just consider  $f_i^+$  since  $f_i^-$  can be  
 163 handled in the same way for its negative. The choice of  $\alpha$  in (1.4) is to make

$$164 \quad (2.2) \quad x_i - y_{\alpha+1} \leq \delta(b-a) < x_i - y_\alpha.$$

165 To accurately approximate  $f_i^+$ , it can be shown that there exist quadrature nodes  
 166  $t_1, \dots, t_p$  and weights  $w_1, \dots, w_p$  with  $p = \mathcal{O}(\log(\epsilon^{-1}) \log(\delta^{-1}))$  such that [2, 7, 13]

$$167 \quad (2.3) \quad \left| \frac{1}{s} - \sum_{k=1}^p w_k e^{-st_k} \right| \leq \epsilon \quad \text{for } s \in [\delta(b-a), b-a].$$

168 (Note that for  $s = x_i - y_j$ , we also have  $s \leq b-a$ .) In practice, the quadrature  
 169 nodes and weights are first found for a single interval  $[1, \delta^{-1}]$  and then adapted to  
 170  $[\delta(b-a), b-a]$  by scaling.

171 With this quadrature approximation, we obtain (1.5)–(1.6). For all  $k = 1, 2, \dots, p$ ,  
 172  $\alpha = 2, \dots, n$ ,  $\beta_{k,\alpha}$  in (1.6) can be precomputed via updates:

$$173 \quad (2.4) \quad \beta_{k,\alpha} = e^{-(y_\alpha - y_{\alpha-1})t_k} \sum_{j=1}^{\alpha-1} z_j e^{-(y_{\alpha-1} - y_j)t_k} + z_\alpha = \beta_{k,\alpha-1} e^{-(y_\alpha - y_{\alpha-1})t_k} + z_\alpha,$$

174 where  $\beta_{k,1} = z_1$  for all  $k$ . The total cost of these updates is  $\mathcal{O}(pn)$ . Accordingly,  $f_i^+$   
 175 for all  $i = 1, 2, \dots, n$  can be approximated using (1.5) in  $\mathcal{O}(pn)$  complexity. Similarly,  
 176 apply the idea to  $f_i^-$ .  $f_i^0$  is directly evaluated, which costs  $\mathcal{O}(mn)$ . With small  $p$  and  
 177  $m$ , the Hilbert transform can be accurately performed in linear complexity.

178 **2.1.2. Matrix form of the SoE expansion.** The fast Hilbert transform in  
 179 [13] as in the previous subsection may be made more intuitive through a matrix form  
 180 of the SoE expansion. For the quadrature weights  $w_k$  and nodes  $t_k$  in (2.3), let

$$181 \quad (2.5) \quad \mathbf{w} = (w_1 \ \cdots \ w_p)^T, \quad \mathbf{t} = (t_1 \ \cdots \ t_p)^T.$$

182 Picking  $\alpha$  as in (2.2), we can rewrite (1.3) as a matrix form

$$183 \quad (2.6) \quad \frac{1}{x_i - y_j} \approx \mathbf{p}_i^T B \mathbf{s}_j \quad \text{with}$$

$$184 \quad (2.7) \quad \mathbf{p}_i = \exp(-(x_i - y_\alpha)\mathbf{t}), \quad B = \text{diag}(\mathbf{w}), \quad \mathbf{s}_j = \exp(-(y_\alpha - y_j)\mathbf{t}).$$

185 Then  $f_i^+$  can be approximated as

$$186 \quad f_i^+ \approx \mathbf{p}_i^T B \boldsymbol{\beta}_\alpha \quad \text{with} \quad \boldsymbol{\beta}_\alpha = (\mathbf{s}_1 \ \cdots \ \mathbf{s}_\alpha) \mathbf{z}_\alpha, \quad \mathbf{z}_\alpha = (z_1 \ \cdots \ z_\alpha)^T.$$

187 We essentially have  $\boldsymbol{\beta}_\alpha = (\beta_{1,\alpha}, \beta_{2,\alpha}, \dots, \beta_{p,\alpha})^T$  with  $\beta_{k,\alpha}$  given in (1.6). Furthermore,  
 188 the updates of  $\beta_{k,\alpha}$  in (2.4) may be written in the following matrix form:

$$189 \quad (2.8) \quad \boldsymbol{\beta}_\alpha = \mathbf{z}_\alpha + (\mathbf{s}_1 \ \mathbf{s}_2 \ \cdots \ \mathbf{s}_{\alpha-1}) \mathbf{z}_{\alpha-1} = \mathbf{z}_\alpha + \Lambda_{\alpha-1} \boldsymbol{\beta}_{\alpha-1} \quad \text{with}$$

$$190 \quad (2.9) \quad \Lambda_{\alpha-1} = \text{diag}(\exp(-(y_\alpha - y_{\alpha-1})\mathbf{t})), \quad \boldsymbol{\beta}_1 = (z_1 \ \cdots \ z_1)^T.$$

191 (Note the notation of scalar vector summation in (2.8).) This clearly illustrates why  
 192  $\boldsymbol{\beta}_\alpha$  for all  $\alpha = 1, 2, \dots, n$  can be precomputed in  $\mathcal{O}(pn)$  complexity.

193 The process of approximating  $f_i^+$ ,  $i = 1, \dots, n$  can then be summarized as follows.

194 1. With  $\boldsymbol{\beta}_1$  in (2.9), for  $j = 2, 3, \dots, n$ , compute

$$195 \quad \boldsymbol{\beta}_j = \mathbf{z}_j + \Lambda_{j-1} \boldsymbol{\beta}_{j-1}.$$

196 2. For  $i = 1, 2, \dots, n$ , pick  $\alpha$  by using  $i$  in (2.2) and compute

$$197 \quad f_i^+ \approx \mathbf{p}_i^T B \boldsymbol{\beta}_\alpha.$$

198 **2.1.3. Structured matrix approximation to the Cauchy kernel matrix.**

199 The approximation (2.6) suggests that the SoE expansion essentially leads to low-  
 200 rank approximations to some blocks of the kernel matrix  $H$  in (1.1) with the Cauchy  
 201 kernel. It further means we can essentially get a structured matrix approximation  
 202 to  $H$ . In this section, we derive this structured approximation, which can reveal the  
 203 actual structured matrix operations beneath the fast Hilbert transform.

204 For the clusters in (1.7), the size  $m$  of each cluster is made small by choosing  
 205 appropriate  $\delta$  in (2.3) such that

$$206 \quad (2.10) \quad x_i - y_j > \delta(b - a) \quad \text{for all} \quad |i - j| \geq m.$$

207 For convenience, we assume that the clusters  $\mathbf{x}_k$  and  $\mathbf{y}_k$  fully interlace in the following  
 208 sense:

$$209 \quad (2.11) \quad x_k^{\max} < y_{k+1}^{\min}, \quad y_k^{\max} < x_{k+1}^{\min},$$

210 where  $x_k^{\max}$  and  $x_k^{\min}$  respectively represent the largest and the smallest points in  $\mathbf{x}_k$ ,  
 211 and  $y_k^{\max}$  and  $y_k^{\min}$  are similarly defined. (If the clusters are not interlaced as this, it  
 212 can actually be shown that the rank structure below becomes simpler.)

213 Then consider a block  $H_{k,l} = \left( \frac{1}{x_i - y_j} \right)_{x_i \in \mathbf{x}_k, y_j \in \mathbf{y}_l}$  of  $H$  defined by the clusters  $\mathbf{x}_k$   
 214 and  $\mathbf{y}_l$ , where  $k > l + 1$ . For each  $x_i \in \mathbf{x}_k, y_j \in \mathbf{y}_l$ , (2.6) holds. It is obvious that we  
 215 can replace  $y_\alpha$  in (2.7) by  $y_{k-2}^{\max}$  so that the approximation (2.6) remains unchanged.  
 216 Accordingly, we get a low-rank approximation

$$217 \quad (2.12) \quad H_{k,l} \approx P_k B S_l,$$

218 where  $P_k$  is formed by stacking the rows  $\mathbf{p}_i^T$  corresponding to all  $x_i \in \mathbf{x}_k$  and  $S_l$   
 219 consists of the columns  $\mathbf{s}_j$  corresponding to all  $y_j \in \mathbf{y}_l$ :

$$220 \quad (2.13) \quad P_k = \left( \exp(-(\mathbf{x}_k - y_{k-2}^{\max})\mathbf{t}^T) \right), \quad S_l = \left( \exp(-\mathbf{t}(y_{k-2}^{\max} - \mathbf{y}_l)^T) \right).$$

221 (Again, here the exponential functions are defined entrywise and are not matrix ex-  
 222 ponentials.) Note that (2.12) holds for all  $1 \leq l \leq k - 2$  and  $P_k$  only depends on  $k$ .  
 223 Thus,  $P_k$  can serve as a column basis matrix for the low-rank approximation of the  
 224 following off-diagonal block row:

$$225 \quad (2.14) \quad (H_{k,1} \quad \cdots \quad H_{k,l} \quad \cdots \quad H_{k,k-2}).$$

See Figure 2.1(i) for an illustration.

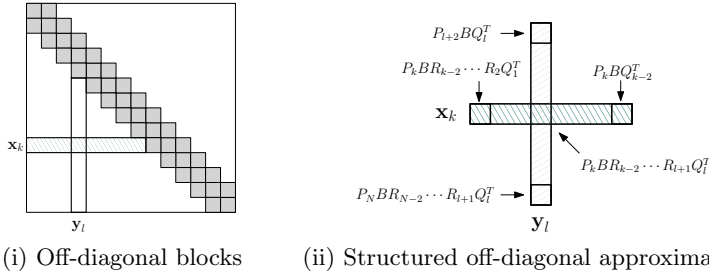


FIG. 2.1. How the off-diagonal blocks (pattern-filled blocks in (i)) of the kernel matrix  $H$  are approximated by low-rank forms from SoE expansions as in (ii).

226

227 Similarly, we may obtain an approximate row basis matrix  $Q_l^T$  for  $H_{k,l}$ , where

$$228 \quad Q_l = \left( \exp(-(y_l^{\max} - \mathbf{y}_l)\mathbf{t}^T) \right).$$

229  $Q_l$  only depends on  $l$  and can serve as a row basis matrix for the low-rank approxi-  
 230 mation of the following off-diagonal block column:

$$231 \quad (2.15) \quad (H_{l+2,l}^T \quad \cdots \quad H_{k,l}^T \quad \cdots \quad H_{N,l}^T)^T.$$

232 Also see Figure 2.1(i). Therefore,  $H_{k,l}$  has an approximation column basis matrix  
 233  $P_k$  and row basis matrix  $Q_l$ . To reflect such a structure for all  $k = 3, \dots, N, l =$   
 234  $1, \dots, k-2$ , we may rewrite (2.12) as

$$235 \quad (2.16) \quad H_{k,l} \approx P_k B R_{k-2} R_{k-3} \cdots R_{l+1} Q_l^T,$$

236 where each  $R_s$  is defined to make  $S_l = R_{k-2} R_{k-3} \cdots R_{l+1} Q_l^T$  and has the form

$$237 \quad (2.17) \quad R_s = \text{diag}(\exp(-(y_s^{\max} - y_{s-1}^{\max})\mathbf{t})).$$

238 At this point, the block row (2.14) and block column (2.15) both appear in nested  
 239 structured forms as illustrated in Figure 2.1(ii). Such a structure is consistent with  
 240 the SSS structure in [10, 11], except that the blocks with  $l = k \pm 1$  are kept dense.

241 Similarly, when  $k+1 < l$ , we may consider

$$242 \quad H_{k,l} = \left( \frac{1}{x_i - y_j} \right)_{x_i \in \mathbf{x}_k, y_j \in \mathbf{y}_l} = - \left( \frac{1}{y_i - x_j} \right)_{y_i \in \mathbf{y}_l, x_j \in \mathbf{x}_k}^T.$$

243 Following the same strategy as above, we can get a structured approximation

$$244 \quad (2.18) \quad H_{k,l} \approx U_k W_{k+1} W_{k+2} \cdots W_{l-2} B V_l^T \quad \text{with}$$

$$245 \quad U_k = -\exp(-(x_k^{\max} - \mathbf{x}_k)\mathbf{t}^T), \quad V_l = \exp(-(\mathbf{y}_l - x_{l-2}^{\max})\mathbf{t}^T),$$

$$246 \quad W_s = \text{diag}(\exp(-(x_s^{\max} - x_{s-1}^{\max})\mathbf{t})).$$

247 To summarize, we have a structured matrix  $A$  that approximates  $H$  as follows:

$$248 \quad (2.19) \quad H_{k,l} \approx A_{k,l} := \begin{cases} D_k, & \text{if } k = l, \\ E_k, & \text{if } k = l - 1, \\ F_{k-1}, & \text{if } k = l + 1, \\ U_k W_{k+1} \cdots W_{l-2} B V_l^T, & \text{if } k < l - 1, \\ P_k B R_{k-2} \cdots R_{l+1} Q_l^T, & \text{if } k > l + 1, \end{cases}$$

249 where  $D_k, E_k$ , and  $F_k$  are equal to the corresponding dense blocks in  $H$  and

$$250 \quad (2.20) \quad \begin{cases} U_k = -\exp(-(x_k^{\max} - \mathbf{x}_k)\mathbf{t}^T), & V_l = \exp(-(\mathbf{y}_l - x_{l-2}^{\max})\mathbf{t}^T), \\ P_k = \exp(-(\mathbf{x}_k - y_{k-2}^{\max})\mathbf{t}^T), & Q_l = \exp(-(\mathbf{y}_l^{\max} - \mathbf{y}_l)\mathbf{t}^T), \\ W_s = \text{diag}(\exp(-(x_s^{\max} - x_{s-1}^{\max})\mathbf{t})), & R_s = \text{diag}(\exp(-(y_s^{\max} - y_{s-1}^{\max})\mathbf{t})). \end{cases}$$

251 To better illustrate the block structure in (2.19), an example is shown as follows:

252

$$253 \quad (2.21) \quad A = \begin{pmatrix} D_1 & E_1 & U_1 B V_3^T & U_1 W_2 B V_4^T & U_1 W_2 W_3 B V_5^T \\ F_1 & D_2 & E_2 & U_2 B V_4^T & U_2 W_3 B V_5^T \\ P_3 B Q_1^T & F_2 & D_3 & E_3 & U_3 B V_5^T \\ P_4 B R_2 Q_1^T & P_4 B Q_2^T & F_3 & D_4 & E_4 \\ P_5 B R_3 R_2 Q_1^T & P_5 B R_3 Q_2^T & P_5 B Q_3^T & F_4 & D_5 \end{pmatrix}.$$

254 The matrix  $A$  has a form as mentioned in [11] that generalizes the classical SSS  
 255 form, and is said to be a *generalized SSS* matrix for convenience. That is, its blocks  
 256 on and below the first block sub-diagonal form a block lower triangular part of an  
 257 SSS matrix and its blocks on and above the first block super-diagonal form a block  
 258 upper triangular part of an SSS matrix. Note that the matrices  $P, Q, U, V, R, W$ , etc.  
 259 that define the generalized SSS form are still the generators of SSS forms so we just

260 call them *SSS generators*. The generators  $P, Q, U, V$  are *basis generators* and  $R, W$   
 261 are *translation generators*. Note that SoE expansions further produce translation  
 262 generators in diagonal forms and with norm bound 1.

263 The generalized SSS form in (2.19) can be quickly multiplied with a vector via  
 264 the SSS matrix-vector multiplication algorithm in [10, 11]. Write  $A(\approx H)$  as

$$265 \quad (2.22) \quad A = A_{\mathbf{D}} + A_{\mathbf{L}} + A_{\mathbf{U}},$$

266 where  $A_{\mathbf{D}}$  is a block banded form corresponding to all the  $D, E$ , and  $F$  generators in  
 267 (2.19), and the nonzero blocks of  $A_{\mathbf{L}}$  and  $A_{\mathbf{U}}$  are respectively block lower and upper  
 268 triangular SSS forms. See Figure 2.2. Each part can be multiplied with a vector  
 269 quickly. To facilitate our later stability analysis, we present the process to compute  
 270  $\mathbf{f}^+ = A_{\mathbf{L}}\mathbf{z}$  with a vector  $\mathbf{z}$  in Algorithm 2.1. Suppose the block sizes is  $m = \mathcal{O}(p)$  and  
 271 the  $W, R$  generators are  $p \times p$ . Then the entire matrix-vector multiplication  $A\mathbf{z}$  costs  
 272  $\mathcal{O}(pm)$  flops.

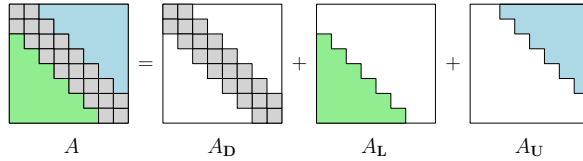


FIG. 2.2. Splitting of a generalized SSS matrix.

---

**Algorithm 2.1** Fast lower-triangular SSS matrix-vector multiplication for  $\mathbf{f}^+$  [11]

---

**Input:** SSS generators  $\{P_k, Q_l, R_s, B\}$  of  $A_{\mathbf{L}}$  and vector  $\mathbf{z}$

**Output:** matrix-vector product  $\mathbf{f}^+ = A_{\mathbf{L}}\mathbf{z}$

- 1: Partition  $\mathbf{z} = (\mathbf{z}_1^T \ \cdots \ \mathbf{z}_N^T)^T$  conformably following the block partitioning of  $A_{\mathbf{L}}$
  - 2:  $\mathbf{v}_1 \leftarrow Q_1^T \mathbf{z}_1$
  - 3: **for**  $k = 2, 3, \dots, N - 2$  **do**
  - 4:      $\mathbf{v}_k \leftarrow Q_k^T \mathbf{z}_k + R_k \mathbf{v}_{k-1};$   $\triangleright$  Backward traversal
  - 5: **end for**
  - 6: **for**  $k = 3, 4, \dots, N$  **do**
  - 7:      $\mathbf{f}_k^+ \leftarrow P_k B \mathbf{v}_{k-2};$   $\triangleright$  Forward traversal
  - 8: **end for**
  - 9:  $\mathbf{f}^+ \leftarrow (0, 0, (\mathbf{f}_3^+)^T \dots, (\mathbf{f}_N^+)^T)^T$   $\triangleright$  Attaching zeros for the zero block rows in  $A_{\mathbf{L}}$
- 

273 *Remark 2.1.* SoE expansions of  $\kappa(x, y)$  like in (1.3) depend on the sign of  $x - y$ .  
 274 An SoE expansion valid for  $x - y > 0$  may need to change the signs of exponentials  
 275 for  $x - y < 0$ . Thus in the splitting (2.22), the subblocks of  $A_{\mathbf{L}}$  and those of  $A_{\mathbf{U}}$   
 276 typically do not share the same block row or column basis matrices.

277 **2.2. Approximations to other kernel matrices.** The generalized SSS structure  
 278 given in (2.19) also holds for kernel matrices  $H$  defined by various other  $\kappa(x, y)$   
 279 that can be approximated by SoE expansions. Some generators may differ. We follow  
 280 similar notation as in the previous subsection and also suppose all  $x_i, y_j \in [a, b]$ .

281 **2.2.1. Gaussian kernels.** In the fast Gauss transform, it needs to quickly eval-  
 282 uate matrix-vector products involving the kernel matrix  $H$  in (1.1) with the Gaussian

283 kernel  $\kappa(x, y) = e^{-(x-y)^2/(4\mu)}$ , where  $\mu > 0$ . SoE expansions for the Gaussian kernel  
 284 based on the Carathéodory-Fejér method [25] have been well studied [21]. They can  
 285 be used to obtain a generalized SSS approximation to  $H$  as follows.

- 286 • Rewrite  $e^{-s^2/(4\mu)}$  through an inverse Laplace transform in the complex plane  
 287 for  $s \in \mathbb{R}$  and then discretize the complex integral to obtain an SoE form:

$$(2.23) \quad e^{-s^2/(4\mu)} = \frac{1}{2\pi\mathbf{i}} \int_{\Gamma} e^z \sqrt{\frac{\pi}{z}} e^{-\sqrt{z/\mu}|s|} dz \approx - \sum_{k=1}^p c_k \sqrt{\frac{\pi}{z_k}} e^{-\sqrt{z_k/\mu}|s|},$$

289 where  $\Gamma$  is a carefully chosen contour in the complex plane and  $c_k, z_k$  are  
 290 generated from an algorithm developed in [26] that computes a nearly optimal  
 291 approximation to  $e^z$  based on the Carathéodory-Fejér method.

- 292 • Substitute  $s = x_i - y_j$  into (2.23) for  $x_i > y_j$  to obtain the SoE approximation

$$(2.23) \quad e^{-(x_i - y_j)^2/(4\mu)} \approx \sum_{k=1}^p w_k e^{-(x_i - y_j)t_k},$$

294 where  $w_k = -c_k \sqrt{\pi/z_k}$  and  $t_k = \sqrt{z_k/\mu}$ .

- 295 • This approximation holds for all  $x_i \in \mathbf{x}, y_j \in \mathbf{y}$  that are used to define  $H$  in  
 296 (1.1). Use it to obtain a generalized SSS approximation similarly to that in  
 297 Section 2.1.3. Since the Gaussian kernel function has no singularity at the  
 298 origin, the dense blocks  $E_k, F_k$  are omitted from the generalized SSS form in  
 299 (2.19). Accordingly, the matrix approximation is given by

$$(2.24) \quad H_{k,l} \approx A_{k,l} = \begin{cases} D_k, & \text{if } k = l, \\ U_k W_{k+1} \cdots W_{l-1} B V_l^T, & \text{if } k \leq l - 1, \\ P_k B R_{k-1} \cdots R_{l+1} Q_l^T, & \text{if } k \geq l + 1, \end{cases}$$

301 where  $D_k$  is equal to the corresponding dense block in  $H$  and

$$(2.25) \quad \begin{cases} U_k = \exp(-(x_k^{\max} - \mathbf{x}_k)\mathbf{t}^T), & V_l = \exp(-(\mathbf{y}_l - x_{l-1}^{\max})\mathbf{t}^T), \\ P_k = \exp(-(\mathbf{x}_k - y_{k-1}^{\max})\mathbf{t}^T), & Q_l = \exp(-(y_l^{\max} - \mathbf{y}_l)\mathbf{t}^T), \\ W_s = \text{diag}(\exp(-(x_s^{\max} - x_{s-1}^{\max})\mathbf{t})), & R_s = \text{diag}(\exp(-(y_s^{\max} - y_{s-1}^{\max})\mathbf{t})). \end{cases}$$

303 Here, the same notation as in (2.5), (1.7), and (2.11) is used (throughout this  
 304 entire paper). Fast evaluation of the Gauss transform is achieved through a  
 305 procedure similar to Algorithm 2.1 with  $\mathcal{O}(pn)$  complexity given the block  
 306 size  $m = \mathcal{O}(p)$ .

307 **2.2.2. Logarithmic kernels.** For the logarithmic kernel  $\log|x - y|$ , one way  
 308 to obtain a generalized SSS approximation to the corresponding kernel matrix  $H$  is  
 309 based on the SoE expansion in [32]. In the following, we let  $\lambda = \delta(b - a)$ .

- 310 • Represent the function  $\log(s)$  for  $s > \lambda$  in an integral form:

$$(2.26) \quad \log(s) = \log(\lambda) + \int_{\lambda}^s \frac{1}{t} dt.$$

- 312 • Apply the SoE expansion in (1.3) to  $1/t$  and integrate explicitly:

$$(2.26) \quad \log(s) \approx \log(\lambda) + \sum_{k=1}^p \frac{w_k}{t_k} e^{-\lambda t_k} + \sum_{k=1}^p -\frac{w_k}{t_k} e^{-s t_k}.$$

- 314 • Replace  $s$  by  $x_i - y_j$  for  $x_i - y_j > \lambda$ :

315 
$$\log(x_i - y_j) \approx c + \sum_{k=1}^p \hat{w}_k e^{-(x_i - y_j)t_k},$$

316 where  $\hat{w}_k = -w_k/t_k$  and  $c = \log(\lambda) + \sum_{k=1}^p \hat{w}_k e^{-\lambda t_k}$ .

- 317 • Accordingly, the generalized SSS approximation to the logarithmic kernel  
318 matrix  $H$  is given by

319 (2.26) 
$$H_{k,l} \approx A_{k,l} = \begin{cases} D_k, & \text{if } k = l, \\ E_k, & \text{if } k = l - 1, \\ F_{k-1}, & \text{if } k = l + 1, \\ c - U_k W_{k+1} \cdots W_{l-2} B V_l^T, & \text{if } k < l - 1, \\ c + P_k B R_{k-2} \cdots R_{l+1} Q_l^T, & \text{if } k > l + 1, \end{cases}$$

320 where  $D_k$ ,  $E_k$ , and  $F_k$  are equal to the corresponding dense blocks in  $H$ ,  
321  $B = -\text{diag}(w_1/t_1, \dots, w_p/t_p)$ , and  $P_k$ ,  $R_s$ ,  $Q_l$ ,  $U_k$ ,  $W_s$ ,  $V_l$  are the same as  
322 those in (2.20).

323 **2.2.3. Square-root kernels.** Next, consider the square-root kernel  $\kappa(x, y) =$   
324  $1/\sqrt{|x^2 - y^2|}$ . Without loss of generality, assume the data sets  $\mathbf{x}$  and  $\mathbf{y}$  are in  $[a, b] \subset$   
325  $\mathbb{R}_+$ . A generalized SSS approximation to the corresponding kernel matrix may be  
326 obtained following an SoE approximation procedure in [32].

- 327 • For  $x_i > y_j$ , write the kernel as the Laplace transform of the modified Bessel  
328 function  $I_0(\cdot)$  of the first kind of order zero:

329 
$$\frac{1}{\sqrt{x_i^2 - y_j^2}} = \int_0^\infty I_0(y_j t) e^{-x_i t} dt = \int_0^\infty \frac{I_0(y_j t)}{e^{y_j t}} e^{-(x_i - y_j)t} dt.$$

330 The last equality is to use the scaled modified Bessel function  $I_0(x)/e^x$  to  
331 avoid computational instability since it is a bounded function on  $\mathbb{R}_+$ .

- 332 • Apply the algorithm provided in [32] to get a generalized Gaussian quadrature  
333 approximation and thus the SoE expansion for  $x_i - y_j > \delta(b - a)$ :

334 
$$\frac{1}{\sqrt{x_i^2 - y_j^2}} = \int_0^\infty \frac{I_0(y_j t)}{e^{y_j t}} e^{-(x_i - y_j)t} dt \approx \sum_{k=1}^p w_k \frac{I_0(y_j t_k)}{e^{y_j t_k}} e^{-(x_i - y_j)t_k},$$

335 where the quadrature weights  $w_k$  and nodes  $t_k$  are close to those in (1.3).

- 336 • Based on this expansion, we get a generalized SSS approximation to the  
337 square-root kernel matrix almost in the same form as in (2.19)–(2.20) other  
338 than slight modifications to some generators:

339 (2.27) 
$$\begin{cases} U_k = \exp(-(x_k^{\max} - \mathbf{x}_k) \mathbf{t}^T) \odot \frac{I_0(\mathbf{x}_k \mathbf{t}^T)}{\exp(\mathbf{x}_k \mathbf{t}^T)}, \\ W_s = \text{diag}(\exp(-(x_s^{\max} - x_{s-1}^{\max}) \mathbf{t})), \\ V_l = \exp(-(\mathbf{y}_l - x_{l-2}^{\max}) \mathbf{t}^T), \\ P_k = \exp(-(\mathbf{x}_k - y_{k-2}^{\max}) \mathbf{t}^T), \\ R_s = \text{diag}(\exp(-(y_s^{\max} - y_{s-1}^{\max}) \mathbf{t})), \\ Q_l = \exp(-(\mathbf{y}_l^{\max} - \mathbf{y}_l) \mathbf{t}^T) \odot \frac{I_0(\mathbf{y}_l \mathbf{t}^T)}{\exp(\mathbf{y}_l \mathbf{t}^T)}, \end{cases}$$

340 where  $\odot$  denotes the Hadamard product.

341 **2.3. SoE approximations for other kernels and higher dimensions.** SoE  
 342 expansions for more kernel functions have been studied in various literatures and gen-  
 343 eralized SSS approximations may be obtained for the corresponding kernel matrices.  
 344 For instance, strategies similar to those in Sections 2.1 can also be applied to other  
 345 functions that can be rewritten as Laplace transforms [7, 32]. Another such example  
 346 is  $\frac{1}{\sqrt{x^2+y^2}}$ , which is useful for designing fast Hankel transforms. An SoE expansion  
 347 can be obtained similarly to those for  $\frac{1}{x-y}$  and  $\frac{1}{\sqrt{x^2-y^2}}$  based on generalized Gauss-  
 348 ian quadratures [31]. This idea can also be extended to find SoE expansions of the  
 349 Cauchy kernel in certain specific regions on the complex plane [31].

350 In [2, 6], some algorithms are designed to obtain SoE expansions for some one-  
 351 dimensional translation-invariant kernels  $\tilde{\kappa}(s) := \kappa(x, y)$  with  $s = x - y$ . The algo-  
 352 rithms are based on solutions of some structured linear system and eigenvalue prob-  
 353 lems. Examples of  $\tilde{\kappa}(s)$  mentioned in [2] include the following:

- 354 •  $1/s^\alpha$  with  $\alpha$  a positive parameter;
- 355 •  $J_0(\alpha s)$  with  $\alpha$  a positive parameter and  $J_0(\cdot)$  the Bessel function of the first  
 356 kind of order zero;
- 357 • the Dirichlet kernel  $\frac{\sin(N\pi s)}{N \sin(\pi s)}$  with  $N \in \mathbb{N}$ ;
- 358 • kernels like  $\log(\sin^2(\pi s))$  and  $\cot(\pi s)$  in harmonic analysis.

359 In [22], a strategy based on Cauchy integration is used to construct SoE expansions  
 360 for general analytical kernel functions  $\tilde{\kappa}(s)$  such as  $s^n$  with odd  $n$ ,  $s^n \log s$  with even  
 361  $n$ ,  $\exp(-\alpha s^2)$ , the Helmholtz kernel  $e^{2\pi i s}/s$ ,  $\sqrt{s^2 + \alpha^2}$ , and  $1/\sqrt{s^2 + \alpha^2}$ , where  $\alpha$  is  
 362 a certain a parameter. The main idea of this method is presented as follows.

- 363 • Apply the Cauchy integral formula to  $\tilde{\kappa}(s)$ :

$$364 \quad (2.28) \quad \tilde{\kappa}(s) = \frac{1}{2\pi i} \int_{\Gamma} \frac{\tilde{\kappa}(z)}{z-s} dz, \quad s \in \mathbb{R},$$

365 where  $\Gamma$  is a Jordan curve in the complex plane and encloses the point  $(s, 0)$ .

- 366 • Partition  $\Gamma$  into pieces  $\Gamma_j$  such that  $\Re(e^{-i\theta_j}(z-s)) > 0$  after  $\theta_j$ -rotation of  
 367  $z-s$  for any  $z \in \Gamma_j$ . Then an SoE expansion is given by

$$368 \quad (2.29) \quad \tilde{\kappa}(s) = \frac{1}{2\pi i} \sum_j e^{-i\theta_j} \int_0^\infty \left( \int_{\Gamma_j} \tilde{\kappa}(z) e^{-tze^{-i\theta_j}} dz \right) e^{tse^{-i\theta_j}} dt \approx \sum_{k=1}^p w_k e^{t_k s},$$

369 where  $w_k$  and  $t_k$  are complex weights and quadrature nodes, respectively, and  
 370  $p = \mathcal{O}\left(\sum_j \log(\max_{z \in \Gamma_j} |\tilde{\kappa}(z)|/\epsilon)\right)$  for a given tolerance  $\epsilon$ .

371 Next, we comment on SoE expansions in higher dimensions. There are different  
 372 ways to get multi-dimensional SoE expansions. As one example, for kernel functions  
 373 like Gaussian in two dimensions, a splitting along the two directions may be made:

$$374 \quad (2.30) \quad e^{-\|\mathbf{c}-\mathbf{s}\|_2^2/(4\mu)} = e^{-(c_1-s_1)^2/(4\mu)} e^{-(c_2-s_2)^2/(4\mu)},$$

375 where  $\mathbf{c} = (c_1, c_2)$  and  $\mathbf{s} = (s_1, s_2)$ . When  $\mathbf{c}$  and  $\mathbf{s}$  are respectively located within two  
 376 clusters of data points, SoE expansions like in (2.23) hold for each dimension if the  
 377 two clusters are separated in that dimension. That is, if an interval for, say, all the  
 378  $c_1$  values does not overlap with an interval for all the  $s_1$  values. If this does not hold  
 379 for a certain dimension, other expansions (like Hermite expansions) may be used [21],  
 380 which leads to a mixture of expansions for the overall kernel.

381 As another example, consider the kernel function  $\frac{1}{\|\mathbf{c}-\mathbf{s}\|_2}$  with  $\mathbf{c} = (c_1, c_2)$  and  
 382  $\mathbf{s} = (s_1, s_2)$  in two dimensions. As SoE expansion may be obtained based on a  
 383 Laplace transform of the Bessel functions for  $c_2 > s_2$  [15]:

$$384 \quad \frac{1}{\|\mathbf{c}-\mathbf{s}\|_2} = \int_0^\infty e^{-t(c_2-s_2)} J_0(t(c_1-s_1)) dt = \frac{1}{\pi} \int_0^\infty e^{-t(c_2-s_2)} \int_0^\pi e^{it(c_1-s_1)\cos\theta} d\theta dt$$

$$385 \quad \approx \sum_{k=1}^p \frac{w_k}{q_k} \sum_{l=1}^{q_k} e^{-t_k[(c_2-s_2)-i(c_1-s_1)\cos(\pi l/q_k)]},$$

386 where  $w_k$  and  $t_k$  are respectively quadrature weights and nodes and  $q_k$  is a positive  
 387 integer depending on  $k$ . The fast algorithm in [15] provides a way to generate  $w_k$  and  
 388  $t_k$  from multipole expansions and is essentially performing a rank-structured matrix-  
 389 vector multiplication like in this paper.

390 There are also other useful techniques for generating SoE expansions for multi-  
 391 dimensional kernels. The Cauchy integration method in [22] for finding SoE ex-  
 392 pansion (like in (2.28)–(2.29) above) can be further extended to analytical kernels  
 393 in higher dimensions. In [19], for the Cauchy kernel in complex regions, a system of  
 394 quadrature weights and nodes is obtained via a conversion from multipole expansions.

395 For multi-dimensional SoE expansions, similarly to the work here, it can be shown  
 396 that fast algorithms like transforms are essentially performed in terms of certain rank-  
 397 structured matrices.

398 **3. Stable transforms via generalized HSS approximations from SoE**  
 399 **expansions.** Fast transforms based on generalized SSS forms essentially compute  
 400 matrix-vector products in a sequential way as in Algorithm 2.1. Later in subsec-  
 401 tion 4.2, we shall see the potential stability limitation. In this section, we give a  
 402 strategy that can significantly enhance the stability by converting the generalized  
 403 SSS form resulting from SoE expansions into a *generalized HSS form*.

404 **3.1. Generalized HSS approximations from SoE expansions.** We say a  
 405 matrix  $A$  a generalized HSS matrix if it can be split as in (2.22) (also see Figure 2.2)  
 406 and the nonzero parts of  $A_L$  and  $A_U$  are triangular lower and upper parts of standard  
 407 HSS matrices, respectively.

408 A brief review of the standard HSS structure in [9, 29] is as follows. An HSS  
 409 matrix  $K$  has a block off-diagonal low-rank form and its blocks follow a partitioning  
 410 strategy as given by a postordered binary tree  $\mathcal{T}$  called HSS tree. To be specific,  
 411 suppose  $\mathcal{T}$  has nodes labeled as  $i = 1, 2, \dots, \sigma$  with  $\sigma$  the root of the HSS tree. Then  
 412 for each non-leaf node  $i$ , the diagonal block  $\mathcal{D}_i$  has the form

$$413 \quad (3.1) \quad \mathcal{D}_i = \begin{pmatrix} \mathcal{D}_{c_1} & \mathcal{U}_{c_1} \mathcal{B}_{c_1} \mathcal{V}_{c_2}^T \\ \mathcal{U}_{c_2} \mathcal{B}_{c_2} \mathcal{V}_{c_1}^T & \mathcal{D}_{c_2} \end{pmatrix},$$

414 where  $c_1, c_2$  are the left and right children of node  $i$  and the calligraphic letters  $\mathcal{D}$ ,  
 415  $\mathcal{U}$ ,  $\mathcal{V}$ ,  $\mathcal{B}$  represent the so-called *HSS generators* so that  $\mathcal{D}_\sigma \equiv K$ .  $\mathcal{U}$ ,  $\mathcal{V}$  are basis  
 416 generators for off-diagonal blocks and further satisfy the following nested relations:

$$417 \quad (3.2) \quad \mathcal{U}_i = \begin{pmatrix} \mathcal{U}_{c_1} \mathcal{R}_{c_1} \\ \mathcal{U}_{c_2} \mathcal{R}_{c_2} \end{pmatrix}, \quad \mathcal{V}_i = \begin{pmatrix} \mathcal{V}_{c_1} \mathcal{W}_{c_1} \\ \mathcal{V}_{c_2} \mathcal{W}_{c_2} \end{pmatrix},$$

418 where  $\mathcal{R}$ ,  $\mathcal{W}$  are known as translation generators.

419 In the following, we convert the generalized SSS approximations in the previous  
 420 section into generalized HSS approximations. More specifically, for an generalized

421 SSS form like in (2.22) and Figure 2.2, we may write the nonzero blocks of, say,  $\mathbf{A}_{\mathbf{L}}$   
 422 in an HSS form. That is, in an HSS construction process, all the generators in (3.1)  
 423 and (3.2) can be explicitly written based on SoE expansions.

424 *Remark 3.1. (Notation)* The HSS construction is essentially for the submatrix of  
 425  $\mathbf{A}_{\mathbf{L}}$  corresponding to block rows 2 to  $N$  and block columns 1 to  $N - 1$ , denoted by  
 426  $\hat{\mathbf{A}}_{\mathbf{L}}$ . Without loss of generality, assume  $N$  in (1.7) satisfies  $N = 2^L + 1$  so that  $\hat{\mathbf{A}}_{\mathbf{L}}$   
 427 has  $2^L$  block rows and  $2^L$  block columns and can be converted into an HSS matrix  
 428 corresponding to an  $L$ -level full binary HSS tree  $\mathcal{T}$ . The HSS form has an  $L$ -level  
 429 hierarchical block structure. The leaf-level blocks correspond to the same partitioning  
 430 as used in the SSS form of  $\hat{\mathbf{A}}_{\mathbf{L}}$ . For convenience, we relabel the point sets associated  
 431 with the block rows and columns. That is, the set  $\mathbf{x}_j$  corresponding to the  $j$ th block  
 432 row of  $\hat{\mathbf{A}}_{\mathbf{L}}$  is relabeled as  $\hat{\mathbf{x}}_i$ , where  $i$  is the node of  $\mathcal{T}$  that is the  $j$ th leaf ordered from  
 433 the left. Then for a non-leaf node  $i$  with children  $c_1$  and  $c_2$ , define  $\hat{\mathbf{x}}_i = \hat{\mathbf{x}}_{c_1} \cup \hat{\mathbf{x}}_{c_2}$ .  
 434 Similarly, define sets  $\hat{\mathbf{y}}_j$ . See Figure 3.1 below. We also introduce notation  $\hat{x}_i^{\max}$  and  
 435  $\hat{x}_i^{\min}$  like in (2.11). We further define the point that immediately precedes  $\hat{x}_i^{\min}$ , if  
 436 any, to be the predecessor of  $\hat{\mathbf{x}}$ , denoted  $\hat{x}_i^{\text{pred}}$ . If this point does not exist (when  $i$  is  
 437 the leftmost node at its level of the tree), then  $\hat{x}_i^{\text{pred}}$  is set to be empty.

438 Without loss of generality, we just show the HSS generators for translation-  
 439 invariant kernels  $\kappa(x, y)$  with SoE expansion

$$440 \quad (3.3) \quad \kappa(x, y) \approx \sum_{k=1}^p w_k e^{-(x-y)t_k} \quad \text{with } x - y \in [\delta(b-a), b-a].$$

441 For other kernels with different SoE expansions, minor modifications may be made to  
 442 the HSS generators.

443 Following (3.3), for any clusters  $\mathbf{x}_k, \mathbf{y}_l$  satisfying  $x_k^{\min} - y_l^{\max} > \delta(b-a)$ , we can  
 444 obtain a low-rank approximation to the corresponding block in the kernel matrix as

$$445 \quad (3.4) \quad (\kappa(x, y))_{x \in \mathbf{x}_k, y \in \mathbf{y}_l} \approx \sum_{k=1}^p w_k e^{-t_k(\mathbf{x}_k - \mathbf{y}_l)} = \sum_{k=1}^p e^{-t_k(\mathbf{x}_k - y_l^{\max})} w_k e^{-t_k(y_l^{\max} - \mathbf{y}_l)}$$

$$446 \quad = \exp(-(\mathbf{x}_k - y_l^{\max})\mathbf{t}^T) B \exp(-\mathbf{t}(y_l^{\max} - \mathbf{y}_l)^T),$$

447 where  $B = \text{diag}(\mathbf{w})$  as before. Now, for  $\mathbf{x}_k, \mathbf{y}_l$  corresponding to any nonzero off-  
 448 diagonal block of  $\hat{\mathbf{A}}_{\mathbf{L}}$ , with the interlacing of the point sets as in (2.11), (3.4) naturally  
 449 holds. Based on this, we can find the low-rank form of the corresponding block of  $\hat{\mathbf{A}}_{\mathbf{L}}$ .

450 The following lemma shows how to obtain the HSS generators.

451 **LEMMA 3.2.** *Suppose the kernel function  $\kappa(x, y)$  satisfies (3.3). Then  $\hat{\mathbf{A}}_{\mathbf{L}}$  can be  
 452 written as an HSS form with generators as follows.*

- 453 • For a leaf node  $i$  of  $\mathcal{T}$ ,

$$454 \quad \mathcal{D}_i = 0, \quad \mathcal{U}_i = \exp(-(\hat{\mathbf{x}}_i - \hat{y}_i^{\text{pred}})\mathbf{t}^T), \quad \mathcal{V}_i = \exp(-(\hat{y}_i^{\max} - \hat{\mathbf{y}}_i)\mathbf{t}^T).$$

- 455 • For a non-leaf node  $i$  with left and right children  $c_1$  and  $c_2$ , respectively,

$$456 \quad \mathcal{B}_{c_1} = 0, \quad \mathcal{B}_{c_2} = B (= \text{diag}(\mathbf{w})).$$

457 If further  $i \neq \sigma$ , then

$$459 \quad \mathcal{R}_{c_1} = I, \quad \mathcal{R}_{c_2} = \text{diag}(\exp(-(\hat{y}_{c_1}^{\max} - \hat{y}_{c_1}^{\text{pred}})\mathbf{t})),$$

$$460 \quad \mathcal{W}_{c_1} = \text{diag}(\exp(-(\hat{y}_{c_2}^{\max} - \hat{y}_{c_1}^{\text{pred}})\mathbf{t})), \quad \mathcal{W}_{c_2} = I.$$

461 *Proof.* Let  $i$  and  $j$  be leaf nodes and respectively be the left and right children of  
 462 their parent  $r$ . Clearly,  $\mathcal{D}_i = \mathcal{D}_j = 0$  by the definition of  $\hat{A}_L$ . According to (3.4), the  
 463 lower off-diagonal block corresponding to  $\hat{\mathbf{x}}_j$  and  $\hat{\mathbf{y}}_i$  has a low-rank approximation

$$464 \quad (3.5) \quad \mathcal{U}_j \mathcal{B}_j \mathcal{V}_i^T = \exp(-(\hat{\mathbf{x}}_j - \hat{\mathbf{y}}_i^{\max}) \mathbf{t}^T) B \exp(-\mathbf{t}(\hat{\mathbf{y}}_i^{\max} - \hat{\mathbf{y}}_i)^T).$$

465 Since  $i$  is the left sibling of  $j$ ,  $\hat{\mathbf{y}}_j^{\text{pred}} = \hat{\mathbf{y}}_i^{\max}$ . We can then let

$$466 \quad (3.6) \quad \mathcal{B}_j = B, \quad \mathcal{U}_j = \exp(-(\hat{\mathbf{x}}_j - \hat{\mathbf{y}}_j^{\text{pred}}) \mathbf{t}^T), \quad \mathcal{V}_i = \exp(-(\hat{\mathbf{y}}_i^{\max} - \hat{\mathbf{y}}_i) \mathbf{t}^T).$$

467 The upper off-diagonal block  $\mathcal{U}_i \mathcal{B}_i \mathcal{V}_j^T = 0$  so we may set

$$468 \quad (3.7) \quad \mathcal{B}_i = 0, \quad \mathcal{U}_i = \exp(-(\hat{\mathbf{x}}_i - \hat{\mathbf{y}}_i^{\text{pred}}) \mathbf{t}^T), \quad \mathcal{V}_j = \exp(-(\hat{\mathbf{y}}_j^{\max} - \hat{\mathbf{y}}_j) \mathbf{t}^T),$$

469 where  $\mathcal{U}_i$  and  $\mathcal{V}_j$  have forms consistent with those in (3.6).

470 If  $i$  and  $j$  are non-leaf sibling nodes, (3.5) still holds so the same forms of  $\mathcal{U}, \mathcal{B}, \mathcal{V}$   
 471 generators as above can be used.

472 We then derive the translation generators  $\mathcal{R}, \mathcal{W}$ . For convenience, suppose  $i$  has  
 473 children  $c_1$  and  $c_2$ , and  $j$  has children  $c_3$  and  $c_4$ , as shown in Figure 3.1. The  $\mathcal{U}, \mathcal{B}, \mathcal{V}$   
 474 generators associated with  $c_1, \dots, c_4$  can be similarly written out.

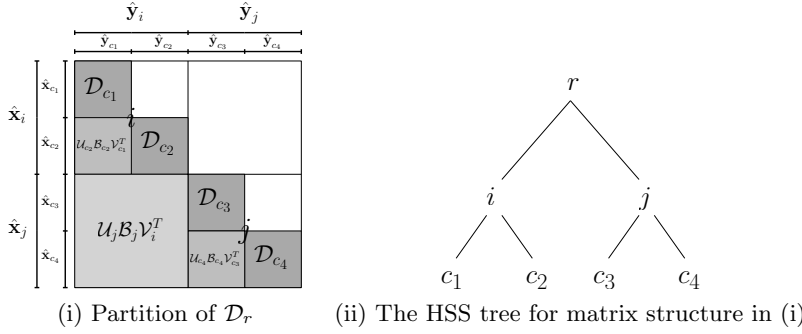


FIG. 3.1. Partitioning of  $\mathcal{D}_r$  corresponding to the tree nodes.

475 Noticing  $\hat{\mathbf{y}}_j^{\text{pred}} = \hat{\mathbf{y}}_{c_3}^{\text{pred}}$  and  $\hat{\mathbf{y}}_i^{\max} = \hat{\mathbf{y}}_{c_2}^{\max}$ , we have

$$476 \quad (3.8) \quad \mathcal{U}_j \mathcal{B}_j \mathcal{V}_i^T = \exp\left(-\begin{pmatrix} \hat{\mathbf{x}}_{c_3} - \hat{\mathbf{y}}_{c_3}^{\text{pred}} \\ \hat{\mathbf{x}}_{c_4} - \hat{\mathbf{y}}_{c_3}^{\text{pred}} \end{pmatrix} \mathbf{t}^T\right) B \exp\left(-\mathbf{t} \begin{pmatrix} \hat{\mathbf{y}}_{c_2}^{\max} - \hat{\mathbf{y}}_{c_1}^T & \hat{\mathbf{y}}_{c_2}^{\max} - \hat{\mathbf{y}}_{c_2}^T \end{pmatrix}\right)$$

$$477 \quad = \begin{pmatrix} \mathcal{U}_{c_3} \\ \mathcal{U}_{c_4} \text{diag}(\exp(-(\hat{\mathbf{y}}_{c_3}^{\max} - \hat{\mathbf{y}}_{c_3}^{\text{pred}}) \mathbf{t})) \end{pmatrix} B \begin{pmatrix} \mathcal{V}_{c_1} \text{diag}(\exp(-(\hat{\mathbf{y}}_{c_2}^{\max} - \hat{\mathbf{y}}_{c_1}^{\max}) \mathbf{t})) \\ \mathcal{V}_{c_2} \end{pmatrix}^T$$

$$478 \quad = \begin{pmatrix} \mathcal{U}_{c_3} \mathcal{R}_{c_3} \\ \mathcal{U}_{c_4} \mathcal{R}_{c_4} \end{pmatrix} B \begin{pmatrix} \mathcal{V}_{c_1} \mathcal{W}_{c_1} \\ \mathcal{V}_{c_2} \mathcal{W}_{c_2} \end{pmatrix}^T.$$

479 Accordingly, we can set

$$480 \quad \mathcal{R}_{c_3} = I, \quad \mathcal{R}_{c_4} = \text{diag}(\exp(-(\hat{\mathbf{y}}_{c_3}^{\max} - \hat{\mathbf{y}}_{c_3}^{\text{pred}}) \mathbf{t})),$$

$$481 \quad \mathcal{W}_{c_1} = \text{diag}(\exp(-(\hat{\mathbf{y}}_{c_2}^{\max} - \hat{\mathbf{y}}_{c_1}^{\max}) \mathbf{t})), \quad \mathcal{W}_{c_2} = I.$$

482 Now, when  $\mathcal{U}_i \mathcal{B}_i \mathcal{V}_j^T$  is considered, we can similarly obtain

$$483 \quad \mathcal{R}_{c_1} = I, \quad \mathcal{R}_{c_2} = \text{diag}(\exp(-(\hat{\mathbf{y}}_{c_1}^{\max} - \hat{\mathbf{y}}_{c_1}^{\text{pred}}) \mathbf{t})),$$

$$484 \quad \mathcal{W}_{c_3} = \text{diag}(\exp(-(\hat{\mathbf{y}}_{c_4}^{\max} - \hat{\mathbf{y}}_{c_3}^{\max}) \mathbf{t})), \quad \mathcal{W}_{c_4} = I.$$

485 To summarize, we get the generators as given in the lemma.  $\square$

486 From this lemma, we can see that the HSS form for  $\hat{A}_{\mathbf{L}}$  further has highly struc-  
 487 tured generators. That is, other than the leaf-level  $\mathcal{U}, \mathcal{V}$  generators, all the other  
 488 generators are diagonal matrices (with some even equal to 0 or  $I$ ).

489 By comparing the HSS generators in [Lemma 3.2](#) with the generalized SSS gener-  
 490 ators in [\(2.19\)](#), we can observe their connections. The HSS generators  $\mathcal{U}$ ,  $\mathcal{V}$ , and  $\mathcal{D}$   
 491 corresponding to the leaf nodes are just the  $P$ ,  $Q$  generators of the SSS form. The  
 492 translation generators  $\mathcal{R}$ ,  $\mathcal{W}$  are basically the products of some  $R$  generators. This  
 493 motivates a way to convert a general SSS form (not necessarily from SoE approxima-  
 494 tions) to an HSS form.

495 *Remark 3.3.* As mentioned in [Remark 3.1](#), when  $i$  is the leftmost node at its level  
 496 of the tree, then  $\hat{x}_i^{\text{pred}}$  is set to be empty. This does not impact the HSS generators  
 497 above needed for multiplying  $\hat{A}_{\mathbf{L}}$  with a vector. The reason is that  $\hat{A}_{\mathbf{L}}$  is block lower  
 498 triangular and any nonzero block  $\mathcal{U}_i \mathcal{B}_i \mathcal{V}_j^T$  in its block lower triangular part satisfies  
 499  $i > j$ . Accordingly, this  $i$  is never the leftmost node at its level.

500 **3.2. Fast transforms via HSS matrix-vector multiplications.** Following  
 501 the splitting [\(2.22\)](#), it suffices to look at the multiplication of  $A_{\mathbf{L}}$  with a vector  $\mathbf{z}$ .  
 502 With the notation in [Remark 3.1](#), this is just to multiply the block lower triangular  
 503 HSS matrix  $\hat{A}_{\mathbf{L}}$  with a part of  $\mathbf{z}$ . We may adapt the HSS matrix-vector multiplication  
 504 algorithm in [\[9, 27\]](#) and further take advantage of the diagonal forms of many gener-  
 505 ators. To facilitate the stability analysis later, we briefly review a telescoping form of  
 506 an HSS matrix and list the main steps of the HSS matrix-vector multiplication.

507 The telescoping form of  $\hat{A}_{\mathbf{L}}$  with generators  $\mathcal{D}, \mathcal{U}, \mathcal{V}, \mathcal{R}, \mathcal{W}, \mathcal{B}$  corresponding to an  
 508  $L$ -level full binary HSS tree looks like [\[23, 27\]](#)

$$509 \quad (3.9) \quad \hat{A}_{\mathbf{L}} = \sum_{k=1}^L \left( \prod_{j=L}^k U^{(j)} \right) B^{(k)} \left( \prod_{j=k}^L (V^{(j)})^T \right) \quad \text{with}$$

$$510 \quad B^{(l)} = \text{diag}(\{\mathbb{B}_i : i \text{ at level } l-1\}),$$

$$511 \quad U^{(l)} = \text{diag}(\{\mathbb{U}_i : i \text{ at level } l\}) \quad \text{and} \quad V^{(l)} = \text{diag}(\{\mathbb{V}_i : i \text{ at level } l\}),$$

512 where

$$513 \quad \mathbb{B}_i = \begin{pmatrix} 0 & \mathcal{B}_{c_1} \\ \mathcal{B}_{c_2} & 0 \end{pmatrix}, \quad i: \text{ non-leaf node with children } c_1, c_2,$$

$$514 \quad \mathbb{U}_i = \begin{cases} \mathcal{U}_i, & i: \text{ leaf,} \\ \begin{pmatrix} \mathcal{R}_{c_1} \\ \mathcal{R}_{c_2} \end{pmatrix}, & i: \text{ non-leaf node,} \end{cases} \quad \mathbb{V}_i = \begin{cases} \mathcal{V}_i, & i: \text{ leaf,} \\ \begin{pmatrix} \mathcal{W}_{c_1} \\ \mathcal{W}_{c_2} \end{pmatrix}, & i: \text{ non-leaf node.} \end{cases}$$

515 To evaluate  $\mathbf{f}^+ = A_{\mathbf{L}} \mathbf{z}$ , we apply the fast HSS matrix-vector multiplication algo-  
 516 rithm in [\[9, 27\]](#) to find  $\hat{\mathbf{f}}^+ = \hat{A}_{\mathbf{L}} \hat{\mathbf{z}}$ , where  $\hat{\mathbf{z}}$  is the portion in  $\mathbf{z}$  corresponding to  $\hat{A}_{\mathbf{L}}$   
 517 and  $\mathbf{f}^+ = \begin{pmatrix} 0 \\ \hat{\mathbf{f}}^+ \end{pmatrix}$ . The main steps are as follows.

518 1. (*Bottom-up traversal*) Let  $\mathbf{z}^{(L+1)} = \hat{\mathbf{z}}$ . For  $l$  from  $L$  to 1, compute

$$519 \quad (3.10) \quad \mathbf{z}^{(l)} = V^{(l)T} \mathbf{z}^{(l+1)}, \quad \mathbf{y}^{(l)} = B^{(l)} \mathbf{z}^{(l)}.$$

520 2. (*Top-down traversal*) Let  $\mathbf{f}^{(0)} = \mathbf{y}^{(1)}$ . For  $l$  from 1 to  $L$ , compute

$$521 \quad (3.11) \quad \mathbf{f}^{(l)} = U^{(l)} \mathbf{f}^{(l-1)} + \mathbf{y}^{(l+1)}.$$

522 Then output  $\hat{\mathbf{f}}^+ = \mathbf{f}^{(L)}$ .

523 **4. Stability analysis for generalized SSS and HSS matrix-vector multi-**  
 524 **plications.** In this section, we discuss the stability of matrix-vector multiplications  
 525 with generalized SSS and HSS forms. The results are presented in a general framework  
 526 so that they hold for all (generalized) SSS and HSS matrices and the fast transforms  
 527 via SoE approximations in this paper may be treated as special cases.

528 **4.1. Motivations and preliminaries.** Our motivations for the stability analy-  
 529 sis are as follows.

- 530 • For an SSS matrix  $A$  with non-orthogonal basis generators, rigorous stability  
 531 analysis for the matrix-vector multiplication has not been done before. The  
 532 work in [1] illustrates the potential instability via an example, although the  
 533 multiplication is structured backward stable in terms of the generators. As  
 534 a remedy, reorthogonalization of basis generators is used to improve stability  
 535 in [1]. Here, we would like to show the stability in terms of  $A$  without or-  
 536 thogonality of the basis generators. The errors may grow exponentially with  
 537 respect to the matrix size  $n$ , which rigorously confirms the stability risk.
- 538 • When  $A$  is written in an HSS form, stability analysis is done in [27] for the  
 539 case again when the basis generators have orthonormal columns. Here, we  
 540 also relax this requirement and show the stability of HSS transforms. Another  
 541 related study is the stability analysis in [24] for the more sophisticated 2D  
 542 FMM. However, the stability study in [24] has a very strict assumption on  
 543 the norm bounds of off-diagonal basis generators at all hierarchical levels. In  
 544 the following, we use separate norm bounds for leaf-level basis generators and  
 545 translation generators, which enables to reveal the importance of the norm  
 546 bounds of translation generators.

547 In the stability analysis below, we study perturbation terms like  $\Delta A$  arising from  
 548 floating point operations involving  $A$ . The analysis will frequently utilize the following  
 549 preliminary lemmas.

550 LEMMA 4.1. [17, p. 69] Let  $A \in \mathbb{R}^{n \times p}$ ,  $\mathbf{z} \in \mathbb{R}^p$ , and

$$551 (4.1) \quad \tau_p = p\epsilon_{\text{mach}}/(1 - p\epsilon_{\text{mach}}),$$

552 where  $\epsilon_{\text{mach}}$  is the machine epsilon. Then the floating point result of the numerical  
 553 matrix-vector multiplication  $A\mathbf{z}$ , denoted  $\text{fl}(A\mathbf{z})$ , satisfies

$$554 \quad \text{fl}(A\mathbf{z}) = (A + \Delta A)\mathbf{z} \quad \text{with} \quad |\Delta A| \leq \tau_p |A|.$$

555 LEMMA 4.2. [17, p. 67] For  $i, j \in \mathbb{N}_+$ ,  $\tau_i$  and  $\tau_j$  defined as in (4.1) satisfy

$$556 \quad i\tau_j \leq \tau_{ij}, \quad \tau_i + \tau_j + \tau_i\tau_j \leq \tau_{i+j},$$

$$557 \quad \tau_i\tau_j \leq \tau_{\min(i,j)} \quad \text{for} \quad \max(i, j)\epsilon_{\text{mach}} \leq 1/2.$$

558 LEMMA 4.3. [24] Let  $P \in \mathbb{C}^{m \times r}$  and  $Q \in \mathbb{C}^{r \times n}$ . Then,

$$559 \quad \|PQ\|_{\max} \leq \|P\|_{\infty} \|Q\|_{\max} \quad \text{and} \quad \|PQ\|_{\max} \leq \|P\|_{\max} \|Q\|_1.$$

560 The following *multi-index* notation (see, e.g., [24]) will be used for convenience.

561 DEFINITION 4.4. (Notation) Let  $\boldsymbol{\xi}$  be a multi-index  $\boldsymbol{\xi} = (\xi_k, \xi_{k+1}, \dots, \xi_l)$  with  $\xi_j \in$   
 562  $\{0, 1\}$  for  $k \leq l$  and  $k, l \in \mathbb{N}$ . Define

$$563 \quad \Delta^{\boldsymbol{\xi}} \left( \prod_{j=k}^l A_j \right) = \prod_{j=k}^l \Delta^{\xi_j} A_j,$$

564 where  $\Delta^0 A_j = A_j$ ,  $\Delta^1 A_j = \Delta A_j$ . Also, denote  $|\xi| = \xi_k + \dots + \xi_l$ . It is easy to verify  
 565 the following identity [24]:

$$566 \quad (4.2) \quad \prod_{j=k}^l (A_j + \Delta A_j) = \prod_{j=k}^l A_j + \sum_{|\xi|=1}^{l-k+1} \Delta^\xi \left( \prod_{j=k}^l A_j \right).$$

567 Throughout the stability analysis, we suppose the generalized SSS/HSS matrices  
 568 meet the following assumptions.

569 ASSUMPTION 4.5. For a generalized SSS or HSS matrix  $A$ , assume the following.

- 570 1. Since the algorithm under consideration is matrix-vector multiplication and  
 571 our focus is the stability study related to off-diagonal structures, we suppose  
 572 all the entries of  $A$  that are not from  $A_{\mathbf{D}}$  are nonzero. (Also note that  $A$  is  
 573 used to approximate kernel matrices in this work.)
- 574 2. The generators of the generalized SSS form defined in (2.19) satisfy

$$575 \quad \|U_k\|_{\max} \leq c_U, \quad \|V_l\|_{\max} \leq c_U, \quad \|P_k\|_{\max} \leq c_U, \quad \|Q_l\|_{\max} \leq c_U,$$

$$576 \quad \|R_s\|_1 \leq c_T, \quad \|W_s^T\|_1 \leq c_T, \quad \|B\|_{\max} \leq c_B |A|_{\min}.$$

577 where  $c_B$  is a constant and  $|A|_{\min}$  is the minimum magnitude of those entries  
 578 of  $A$  that are not from  $A_{\mathbf{D}}$ . For convenience, we assume that  $U_k, V_l, P_k, Q_l$   
 579 have sizes  $m \times p$  and  $R_s, W_s, B$  have sizes  $p \times p$ .

- 580 3. The generators of the generalized HSS form like in (3.1) and (3.2) satisfy

$$581 \quad \|\mathcal{U}_i\|_{\max} \leq c_U, \quad \|\mathcal{V}_i\|_{\max} \leq c_U, \quad \|\mathcal{R}_i\|_{\infty} \leq c_T, \quad \|\mathcal{W}_i\|_{\infty} \leq c_T,$$

$$582 \quad \|\mathcal{B}_i\|_{\max} \leq c_B |A|_{\min}.$$

583 Note that for  $A$  in (2.22), the generators for  $A_{\mathbf{L}}$  and  $A_{\mathbf{U}}$  may be differ-  
 584 ent. Nevertheless, we suppose all the relevant generators satisfy these norm  
 585 bounds. For convenience, we also assume that the HSS tree  $\mathcal{T}$  is a full binary  
 586 tree with  $L (\approx \log N)$  levels, where  $N$  is the number of leaves in  $\mathcal{T}$ . Also, we  
 587 assume that  $\mathcal{U}_i, \mathcal{V}_i$  have sizes  $m \times p$  and  $\mathcal{R}_i, \mathcal{W}_i, \mathcal{B}_i$  have sizes  $p \times p$ .

- 588 4. For  $m, p$ , and  $N$ , we assume that  $p \leq m$  as in typical structured matrix  
 589 algorithms (so that the leaf-level block sizes are not too small to have any  
 590 cost saving), and assume  $n_{\epsilon_{\text{mach}}} \approx N\tau_m \ll 1$  as in typical backward stability  
 591 analysis. (Note  $n = Nm$ .)

592 Remark 4.6. To validate such assumptions within the context of this paper, we  
 593 take the Cauchy kernel matrices in Section 2.1 as an example, where the generalized  
 594 HSS matrix is constructed in Lemma 3.2 with the SoE expansion in the form of (3.3)  
 595 and further satisfying  $w_k, t_k \geq 0$  for all  $k$ . (The assumptions can be similarly validated  
 596 for the other kernel matrices.) Notice that the generators  $\mathcal{U}, \mathcal{V}, \mathcal{R}, \mathcal{W}$  have entries with  
 597 magnitudes bounded by 1. In this case,  $c_U = c_T = 1$ . For the  $\mathcal{B}$  generators,

$$598 \quad (4.3) \quad \|\mathcal{B}_i\|_{\max} = \max_{k=1, \dots, p} |w_k| \leq \sum_{k=1}^p w_k \leq \sum_{k=1}^p w_k e^{[(b-a)-|x-y|]t_k}$$

$$599 \quad \leq c_B \sum_{k=1}^p w_k e^{-|x-y|t_k} \quad \text{with} \quad c_B := \max_{k=1, \dots, p} e^{(b-a)t_k}.$$

600 Since this holds for all  $|x - y| \geq \delta(b - a)$ , we get  $\|\mathcal{B}_i\|_{\max} \leq c_B |A|_{\min}$ . Note (3.3)  
 601 means  $|A|_{\min} = \min_{|x-y| \geq \delta(b-a)} \sum_{k=1}^p w_k e^{-|x-y|t_k}$ .

602 We then present the stability analysis in the next two subsections.

603 **4.2. Stability analysis for generalized SSS matrix-vector multiplica-**  
 604 **tions.** The fast transforms in Section 2 are done through generalized SSS matrix-  
 605 vector multiplications following the splitting (2.22):  $Az = A_{\mathbf{D}}z + A_{\mathbf{L}}z + A_{\mathbf{U}}z$ , where  
 606  $A_{\mathbf{D}}z$  is computed through a direct block banded matrix-vector multiplication,  $A_{\mathbf{L}}z$  is  
 607 computed following Algorithm 2.1, and  $A_{\mathbf{U}}z$  is computed similarly to  $A_{\mathbf{L}}z$  because of  
 608 the structural symmetry. Hence, it suffices to analyze the stability of  $\mathbf{f}^+ = A_{\mathbf{L}}z$ .

609 Suppose  $\text{fl}(\mathbf{f}^+) = (A_{\mathbf{L}} + \Delta\tilde{A}_{\mathbf{L}})z$  with  $\Delta\tilde{A}_{\mathbf{L}}$  the perturbation due to the numerical  
 610 computation. For a block  $A_{k,l}$  with  $k > l + 1$  like in (2.19), the perturbation  $\Delta\tilde{A}_{k,l}$  (a  
 611 block of  $\Delta\tilde{A}_{\mathbf{L}}$ ) is produced from  $\text{fl}(\mathbf{f}_k^+) = \sum_{l=1}^{k-2} (A_{k,l} + \Delta\tilde{A}_{k,l})z_l$  via the two traversals  
 612 in Algorithm 2.1. Our task is to find an entrywise bound for each such  $\Delta\tilde{A}_{k,l}$ . Two  
 613 lemmas in the following measure the perturbations in these traversals and will be used  
 614 in the proof of the main Theorem 4.9. The proofs of these lemmas are included in  
 615 Appendix A. The discussions below involve the following notation from [24]:

$$616 \quad \prod_{s=k}^{\geq l} A_s = \begin{cases} A_k A_{k-1} \cdots A_l, & k \geq l, \\ I, & k < l. \end{cases}$$

617 LEMMA 4.7. Suppose  $A$  in the form of (2.22) is a generalized SSS matrix satisfy-  
 618 ing the assumptions in Assumption 4.5. Then in the evaluation of  $\mathbf{f}^+ = A_{\mathbf{L}}z$ ,  $\text{fl}(\mathbf{v}_k)$   
 619 produced via the backward traversal stage of Algorithm 2.1 for  $1 \leq k \leq N - 2$  satisfies

$$620 \quad (4.4) \quad \text{fl}(\mathbf{v}_k) = \mathbf{v}_k + \Delta\mathbf{v}_k \quad \text{with} \quad \Delta\mathbf{v}_k = \sum_{l=1}^k \left[ \sum_{|\xi|=1}^{k-l+1} \Delta^\xi \left( \left( \prod_{s=k}^{\geq l+1} \tilde{R}_s \right) \tilde{Q}_l^T \right) \right] z_l,$$

621 where

$$622 \quad (4.5) \quad \Delta^\xi \tilde{Q}_l^T := \begin{cases} Q_l^T, & \xi = 0, \\ \Delta Q_l^T + \Delta Y_l Q_l^T + \Delta Y_l \Delta Q_l^T, & \xi = 1, \end{cases} \quad \text{with} \quad |\Delta Q_l^T| \leq \tau_m |Q_l^T|,$$

$$623 \quad (4.6) \quad \Delta^\xi \tilde{R}_s := \begin{cases} R_s, & \xi = 0, \\ \Delta R_s + \Delta Y_s R_s + \Delta Y_s \Delta R_s, & \xi = 1, \end{cases} \quad \text{with} \quad |\Delta R_s| \leq \tau_p |R_s|,$$

624  $|\Delta Y_l| \leq \epsilon_{\text{mach}} I$ , and the notation in (4.1) is used. Besides, we have

$$625 \quad \|\Delta^1 \tilde{Q}_l^T\|_1 \leq pc_U \tau_{3m}, \quad \|\Delta^1 \tilde{R}_s\|_1 \leq c_T \tau_{3p}.$$

626 LEMMA 4.8. Suppose  $A$  in the form of (2.22) is a generalized SSS matrix satisfy-  
 627 ing the assumptions in Assumption 4.5. Then in the evaluation of  $\mathbf{f}^+ = A_{\mathbf{L}}z$ ,  $\text{fl}(\mathbf{f}_k^+)$   
 628 produced after the forward traversal in Algorithm 2.1 for  $3 \leq k \leq N$  satisfies

$$629 \quad \text{fl}(\mathbf{f}_k^+) = \mathbf{f}_k^+ + \Delta\mathbf{f}_k^+ \quad \text{with} \quad \Delta\mathbf{f}_k^+ = \sum_{l=1}^{k-2} \Delta\tilde{A}_{k,l} z_l,$$

630 where

$$631 \quad \Delta\tilde{A}_{k,l} = \sum_{|\xi|=1}^{k-l+1} \Delta^\xi \left[ P_k B \left( \prod_{s=k-2}^{\geq l+1} \tilde{R}_s \right) \tilde{Q}_l^T \right], \quad |\Delta P_k| \leq \tau_p |P_k|, \quad |\Delta B| \leq \tau_p |B|,$$

632 and  $\Delta^\xi \tilde{R}_s$  and  $\Delta^\xi \tilde{Q}_l^T$  are respectively defined in (4.5) and (4.6). Besides,

$$633 \quad (4.7) \quad |\Delta\tilde{A}_{k,l}| \leq \frac{4}{3} (k-l+1) \tau_{3m} p^2 c_B c_U^2 c_T^{k-l-2} |A_{k,l}| \quad \text{for} \quad k > l + 1.$$

634 We can now inspect the stability of generalized SSS matrix-vector multiplications.

635 **THEOREM 4.9.** *Suppose  $A$  in the form of (2.22) is a generalized SSS matrix sat-*  
 636 *isfying the assumptions in Assumption 4.5. Then the matrix-vector multiplication of*  
 637  *$A$  with a vector  $\mathbf{z}$  via Algorithm 2.1 satisfies*

$$638 \quad \text{fl}(\mathbf{Az}) = (A + \Delta A)\mathbf{z} \quad \text{with}$$

$$639 \quad |\Delta A| \leq \max\{1, \frac{4}{3}Np^2c_Bc_U^2 \max\{1, c_T^{N-3}\}\} \tau_{3m+4}|A|.$$

640 *Proof.* We discuss the perturbations to a nonzero block  $A_{k,l}$  from  $A_{\mathbf{L}}$ ,  $A_{\mathbf{U}}$ , or  $A_{\mathbf{D}}$   
 641 in (2.22) due to the multiplications  $\mathbf{f}^0 = A_{\mathbf{D}}\mathbf{z}$ ,  $\mathbf{f}^+ = A_{\mathbf{L}}\mathbf{z}$ , and  $\mathbf{f}^- = A_{\mathbf{U}}\mathbf{z}$ , respectively.  
 642 According to Lemma 4.1,

$$643 \quad \text{fl}(\mathbf{f}^0) = (A_{\mathbf{D}} + \Delta\tilde{A}_{\mathbf{D}})\mathbf{z},$$

644 where  $\Delta\tilde{A}_{\mathbf{D}}$  has the same block structure as  $A_{\mathbf{D}}$  and its blocks satisfy  $|\Delta\tilde{A}_{k,l}| \leq$   
 645  $\tau_{3m}|A_{k,l}|$  since there are at most  $3m$  nonzero columns in each block row of  $A_{\mathbf{D}}$ .

646 Next,

$$647 \quad \text{fl}(\mathbf{f}^+) = (A_{\mathbf{L}} + \Delta\tilde{A}_{\mathbf{L}})\mathbf{z},$$

648 where  $\Delta\tilde{A}_{\mathbf{L}}$  has the same block structure as  $A_{\mathbf{L}}$  and its blocks  $\Delta\tilde{A}_{k,l}$  satisfy (4.7) in  
 649 Lemma 4.8. Then, by the structure symmetry between  $A_{\mathbf{U}}$  and  $A_{\mathbf{L}}$ , Lemma 4.7 and  
 650 Lemma 4.8 also apply to  $A_{k,l}$  from  $A_{\mathbf{U}}$  or when  $k < l - 1$ . Thus,

$$651 \quad \text{fl}(\mathbf{f}^-) = (A_{\mathbf{U}} + \Delta\tilde{A}_{\mathbf{U}})\mathbf{z},$$

652 where  $\Delta\tilde{A}_{\mathbf{U}}$  has the same block structure as  $A_{\mathbf{U}}$  and its blocks  $\Delta\tilde{A}_{k,l}$  satisfy the same  
 653 bound (4.7) in Lemma 4.8 when  $k > l + 1$ . Thus, for any  $1 \leq k, l \leq N$ ,

$$654 \quad (4.8) \quad |\Delta\tilde{A}_{k,l}| \leq \begin{cases} \tau_{3m}|A_{k,l}|, & |k-l| \leq 1, \\ \frac{4}{3}(|k-l|+1)p^2c_Bc_U^2c_T^{|k-l|-2}\tau_{3m}|A_{k,l}|, & \text{otherwise.} \end{cases}$$

655 In the final summation stage, we then have

$$656 \quad \text{fl}(\mathbf{Az}) = \text{fl}(\text{fl}(\mathbf{f}^0) + \text{fl}(\mathbf{f}^+) + \text{fl}(\mathbf{f}^-))$$

$$657 \quad (4.9) \quad = (I + \Delta f_2) \left( (I + \Delta f_1)(\mathbf{f}^0 + \Delta\tilde{A}_{\mathbf{D}}\mathbf{z} + \mathbf{f}^+ + \Delta\tilde{A}_{\mathbf{L}}\mathbf{z}) + \mathbf{f}^- + \Delta\tilde{A}_{\mathbf{U}}\mathbf{z} \right),$$

658 where  $\Delta f_1$  results from the floating point addition  $\text{fl}(\mathbf{f}^0) + \text{fl}(\mathbf{f}^+)$  and  $\Delta f_2$  results from  
 659 the further floating point addition of  $\text{fl}(\mathbf{f}^-)$  and they are diagonal matrices satisfying  
 660  $|\Delta f_1| \leq \epsilon_{\text{mach}}I$ ,  $|\Delta f_2| \leq \epsilon_{\text{mach}}I$ .

661 Let

$$662 \quad (4.10) \quad \Delta\tilde{A} = \Delta\tilde{A}_{\mathbf{D}} + \Delta\tilde{A}_{\mathbf{L}} + \Delta\tilde{A}_{\mathbf{U}}.$$

663 Then

$$664 \quad (4.11) \quad \text{fl}(\mathbf{Az}) = \mathbf{f}^0 + \mathbf{f}^+ + \mathbf{f}^- + (\Delta A)\mathbf{z} = \mathbf{Az} + (\Delta A)\mathbf{z},$$

$$665 \quad (4.12) \quad \Delta A = \Delta\tilde{A} + \Delta f_2(A + \Delta\tilde{A}) + (\Delta f_2\Delta f_1 + \Delta f_1)(A_{\mathbf{D}} + A_{\mathbf{L}} + \Delta\tilde{A}_{\mathbf{D}} + \Delta\tilde{A}_{\mathbf{L}}).$$

666 Since  $\Delta f_1$  and  $\Delta f_2$  are diagonal and  $A_{\mathbf{D}}$  and  $A_{\mathbf{L}}$  have non-overlapping nonzero pat-  
667 terns, we then have

$$\begin{aligned}
668 \quad (4.13) \quad |\Delta A| &\leq |\Delta \tilde{A}| + |\Delta f_2|(|A| + |\Delta \tilde{A}|) \\
669 &\quad + (|\Delta f_2||\Delta f_1| + |\Delta f_1|)(|A_{\mathbf{D}}| + |A_{\mathbf{L}}| + |\Delta \tilde{A}_{\mathbf{D}}| + |\Delta \tilde{A}_{\mathbf{L}}|) \\
670 &\leq |\Delta \tilde{A}| + \epsilon_{\text{mach}}(|A| + |\Delta \tilde{A}|) + (\epsilon_{\text{mach}} + \epsilon_{\text{mach}}^2)(|A| + |\Delta \tilde{A}|) \\
671 &\leq (2\epsilon_{\text{mach}} + \epsilon_{\text{mach}}^2)|A| + (1 + \epsilon_{\text{mach}})^2|\Delta \tilde{A}| \\
672 &\leq (\tau_2 + (1 + \tau_2) \max\{1, \frac{4}{3}Np^2c_Bc_U^2 \max\{1, c_T^{N-3}\}\}\tau_{3m})|A| \\
673 &\leq \max\{1, \frac{4}{3}Np^2c_Bc_U^2 \max\{1, c_T^{N-3}\}\}\tau_{3m+4}|A|,
\end{aligned}$$

674 where the last two steps follow from [Lemma 4.2](#) and [\(4.8\)](#).  $\square$

675 [Theorem 4.9](#) shows that generalized SSS transforms may potentially have expo-  
676 nential error growth with respect to  $N$  when  $c_T$ , the norm bound of the translation  
677 generators, is larger than 1. (Note  $N$  is proportional to  $n$ .) Translation generators  
678 with large norms may cause instability. On the other hand, SoE expansions provide  
679 an effective way to resolve this issue by producing nice bounds for the translation  
680 generators.

681 **COROLLARY 4.10.** *Suppose the generators of the generalized SSS matrix  $A$  are*  
682 *produced via SoE expansions as in [\(3.4\)](#) so that the generators further satisfy  $c_T =$*   
683  *$c_U = 1$ . Then, generalized SSS matrix-vector multiplications via [Algorithm 2.1](#) satisfy*

$$684 \quad \mathfrak{fl}(A\mathbf{z}) = (A + \Delta A)\mathbf{z} \quad \text{with} \quad |\Delta A| \leq \max\{1, \frac{4}{3}Np^2c_B\}\tau_{3m+4}|A|.$$

685 In this corollary, the error grows at most linearly with respect to  $N$ .

686 **4.3. Stability analysis for generalized HSS matrix-vector multiplica-**  
687 **tions.** The previous subsection shows the importance of controlling the norms of  
688 translation generators. In practice, it is possible for structured representations to  
689 have translation operators with norms larger than 1. In this subsection, we consider  
690 another important factor that impacts the stability of transforms: the algorithm ar-  
691 chitecture. As mentioned in [\[27, 28\]](#), hierarchical structured (like HSS) algorithms  
692 can further reduce the length of the error propagation path or the number of times  
693 the error gets magnified by.

694 [Theorem 4.13](#) below shows how the HSS architecture benefits the stability and  
695 can be shown based on the following two lemmas, which are proved in [Appendix A](#).

696 **LEMMA 4.11.** *Suppose  $A$  in the form of [\(2.22\)](#) is a generalized HSS matrix sat-*  
697 *isfying the assumptions in [Assumption 4.5](#). Then in the evaluation of  $\hat{\mathbf{f}}^+ = \hat{A}_{\mathbf{L}}\hat{\mathbf{z}}$ ,*  
698  *$\mathfrak{fl}(\mathbf{y}^{(i)})$  produced via the bottom-up traversal in [\(3.10\)](#) for  $1 \leq i \leq L$  satisfies*

$$699 \quad (4.14) \quad \mathfrak{fl}(\mathbf{y}^{(i)}) = \mathbf{y}^{(i)} + \Delta \mathbf{y}^{(i)} \quad \text{with} \quad \Delta \mathbf{y}^{(i)} = \left( \sum_{|\xi|=1}^{L-i+2} \Delta^\xi \left( B^{(i)} \prod_{j=i}^L (V^{(j)})^T \right) \right) \hat{\mathbf{z}},$$

700 where  $|\Delta B^{(i)}| \leq \tau_p |B^{(i)}|$  and  $|(\Delta V^{(j)})^T| \leq \tau |V^{(j)}|^T$  for  $\tau = \max\{\tau_m, \tau_{2p}\}$ . Besides,  
701  $\|\Delta^\xi(\prod_{j=i}^L (V^{(j)})^T)\|_1 \leq pc_U c_T^{L-i} \tau_{2m}^{|\xi|}$ .

702 LEMMA 4.12. Suppose  $A$  in the form of (2.22) is a generalized HSS matrix satis-  
 703 fying the assumptions in Assumption 4.5. Then in the evaluation of  $\hat{\mathbf{f}}^+ = \hat{A}_{\mathbf{L}}\hat{\mathbf{z}}$ ,  $\text{fl}(\hat{\mathbf{f}}^+)$   
 704 produced after the top-down traversal in (3.11) satisfies

$$705 \quad (4.15) \quad \text{fl}(\hat{\mathbf{f}}^+) = (\hat{A}_{\mathbf{L}} + \Delta\hat{A}_{\mathbf{L}})\hat{\mathbf{z}} \quad \text{with} \quad \Delta\hat{A}_{\mathbf{L}} = \sum_{k=1}^L \Delta\hat{A}_{\mathbf{L}}^{(k)},$$

706 where

$$707 \quad (4.16) \quad \Delta\hat{A}_{\mathbf{L}}^{(k)} = \sum_{|\xi|=1}^{2L-2k+3} \Delta^\xi \left( \left( \prod_{j=L}^{\geq k} \tilde{U}^{(j)} \right) B^{(k)} \left( \prod_{j=k}^L (V^{(j)})^T \right) \right),$$

708  $\Delta V^{(j)}$  and  $\Delta B^{(k)}$  are defined in Lemma 4.11, and

$$709 \quad \Delta^\xi \tilde{U}^{(j)} := \begin{cases} U^{(j)}, & \text{if } \xi = 0, \\ \Delta U^{(j)} + U^{(j)}\Delta Z^{(j-1)} + \Delta U^{(j)}\Delta Z^{(j-1)}, & \text{if } \xi = 1, \end{cases} \quad \text{with}$$

$$710 \quad |\Delta Z^{(j)}| \leq \epsilon_{\text{mach}}I, \quad |\Delta U^{(j)}| \leq \tau_p |U^{(j)}|.$$

711 Besides,

$$712 \quad (4.17) \quad |\Delta\hat{A}_{\mathbf{L}}| \leq \frac{4}{3}(2L+1)p^2 c_B c_U^2 \max\{1, c_T^{2L-2}\} \tau_{3m} |\hat{A}_{\mathbf{L}}|.$$

713 We can then show the backward stability of transforms with generalized HSS  
 714 matrix-vector multiplications.

715 THEOREM 4.13. Suppose  $A$  in the form of (2.22) is a generalized HSS matrix  
 716 satisfying the assumptions in Assumption 4.5. Assume the matrix-vector multiplica-  
 717 tion of  $A$  with a vector  $\mathbf{z}$  is performed with  $A_{\mathbf{L}}\mathbf{z}$  computed via the traversals in (3.10)  
 718 and (3.11),  $A_{\mathbf{U}}\mathbf{z}$  computed similarly based on structure symmetry, and  $A_{\mathbf{D}}\mathbf{z}$  computed  
 719 directly. Then

$$720 \quad \text{fl}(A\mathbf{z}) = (A + \Delta A)\mathbf{z} \quad \text{with}$$

$$721 \quad |\Delta A| \leq \max\{1, \frac{4}{3}(2L+1)p^2 c_B c_U^2 \max\{1, c_T^{2L-2}\}\} \tau_{3m+4} |A|.$$

722 *Proof.* The framework of the stability analysis is similar to that in the proof of  
 723 Theorem 4.9. For convenience, we follow the same definitions and notation as in the  
 724 proof of Theorem 4.9 up to (4.12).

725 Note that  $\Delta\hat{A}_{\mathbf{L}}$  and  $\Delta\tilde{A}_{\mathbf{U}}$  in (4.10) are perturbations generated from HSS matrix-  
 726 vector multiplications that have the same nonzero structure as  $A_{\mathbf{L}}$  and  $A_{\mathbf{U}}$ , respec-  
 727 tively. According to (4.17) in Lemma 4.12, we have

$$728 \quad |\Delta\tilde{A}_{\mathbf{L}}| \leq \frac{4}{3}(2L+1)p^2 c_B c_U^2 \max\{1, c_T^{2L-2}\} \tau_{3m} |A_{\mathbf{L}}|.$$

729 By the structure symmetry between  $A_{\mathbf{U}}$  and  $A_{\mathbf{L}}$ , Lemmas 4.11 and 4.12 also apply  
 730 to  $\Delta\tilde{A}_{\mathbf{U}}$ . Then,

$$731 \quad |\Delta\tilde{A}_{\mathbf{U}}| \leq \frac{4}{3}(2L+1)p^2 c_B c_U^2 \max\{1, c_T^{2L-2}\} \tau_{3m} |A_{\mathbf{U}}|.$$

732 Since the nonzero patterns of  $\Delta\tilde{A}_{\mathbf{D}}$ ,  $\Delta\tilde{A}_{\mathbf{L}}$ , and  $\Delta\tilde{A}_{\mathbf{U}}$  do not overlap, we then have

$$733 \quad |\Delta\tilde{A}| \leq \max\{1, \frac{4}{3}(2L+1)p^2c_Bc_U^2 \max\{1, c_T^{2L-2}\}\tau_{3m}|A|,$$

734 Accordingly, by (4.13), we have

$$\begin{aligned} 735 \quad |\Delta A| &\leq |\Delta\tilde{A}| + (2\epsilon_{\text{mach}} + \epsilon_{\text{mach}}^2)(|A| + |\Delta\tilde{A}|) \\ 736 \quad &\leq (\tau_2 + (1 + \tau_2) \max\{1, \frac{4}{3}(2L+1)p^2c_Bc_U^2 \max\{1, c_T^{2L-2}\}\tau_{3m})|A| \\ 737 \quad &\leq \max\{1, \frac{4}{3}(2L+1)p^2c_Bc_U^2 \max\{1, c_T^{2L-2}\}\tau_{3m+4}|A|. \quad \square \end{aligned}$$

738 **Theorem 4.13** shows that the generalized HSS transform is backward stable. This  
739 holds even if the norm bound  $c_T$  of the translation generators is larger than 1. In  
740 that case, the backward error has polynomial (instead of exponential) growth. With  
741 further control on the norm bounds of the generators (via the SoE expansions), the  
742 error propagation of the generalized HSS transform can be even reduced to poly-  
743 logarithmic.

744 **COROLLARY 4.14.** *Suppose the generators of the generalized HSS matrix  $A$  are*  
745 *produced via the SoE expansions as in (3.4) so that the generators further satisfy  $c_T =$*   
746  *$c_U = 1$ . Then the generalized HSS matrix-vector multiplication as in [Theorem 4.13](#)*  
747 *satisfies*

$$748 \quad \text{fl}(A\mathbf{z}) = (A + \Delta A)\mathbf{z} \quad \text{with} \quad |\Delta A| \leq \max\{1, \frac{4}{3}(2L+1)p^2c_B\}\tau_{3m+4}|A|.$$

749 **Remark 4.15. (Key observations)** The studies in this section provide some useful  
750 insights into the stability of rank-structured algorithms like matrix-vector multiplica-  
751 tions. Two key components play crucial roles in the stability: *algorithm architecture*  
752 and *norm bounds of translation generators*. As compared with sequential architec-  
753 tures, hierarchical architectures help reduce the length of the error propagation path  
754 from  $\mathcal{O}(n)$  to  $\mathcal{O}(\log n)$ . See [Theorems 4.9](#) and [4.13](#). Smaller norm bounds for transla-  
755 tion generators yield lower error growth factors. Depending on these two components,  
756 the possible error growth patterns are as follows:

- 757 • exponential (e.g., generalized SSS with  $c_T > 1$  as in [Theorem 4.9](#));
- 758 • polynomial (e.g., generalized SSS with  $c_T = 1$  as in [Corollary 4.10](#), and HSS  
759 with  $c_T > 1$  as in [Theorem 4.13](#));
- 760 • poly-logarithmic (e.g., generalized HSS with  $c_T = 1$  as in [Corollary 4.14](#)).

761 Thus, to perform the fast transforms in this paper, using generalized HSS structures  
762 derived from SoE expansions potentially has the best stability.

763 **5. Numerical experiments.** In this section, we use some numerical exper-  
764 iments to illustrate the stability of transformations via generalized SSS and HSS  
765 matrix-vector multiplications. We also confirm the high accuracy and efficiency of  
766 the generalized HSS matrix-vector multiplication.

767 Four kernel functions in Section 2 are considered in the tests: Cauchy ( $1/(x-y)$ ),  
768 Gaussian ( $e^{-(x-y)^2}$ ), logarithmic ( $\log|x-y|$ ), and square-root ( $1/\sqrt{|x^2-y^2|}$ ). For  
769 convenience, we let the data sets  $\mathbf{x}$  and  $\mathbf{y}$  be identical. Whenever a diagonal entry  
770  $\kappa(x_i, x_i)$  is undefined, it is set to be zero. This does not really matter for the stability  
771 tests related to off-diagonal structures.

772 For each kernel matrix, SoE expansions are used to obtain a generalized SSS or  
 773 HSS approximation  $A$ . For SoE approximations to Cauchy, logarithmic, and square-  
 774 root kernels, a parameter  $\delta$  like in (2.3) is needed to determine the valid intervals  
 775 of the approximations. With the finest-level block size  $m$  fixed, appropriate  $\delta$  and  
 776 the corresponding quadrature nodes and weights are chosen for different data sizes  
 777  $n$  to meet conditions (2.10)–(2.11). Given a tolerance  $\epsilon = 10^{-15}$  of SoE approxi-  
 778 mations, some sets of quadrature nodes and weights for  $\delta = \frac{1}{4^k}$ ,  $k = 1, 2, \dots, 10$  are  
 779 precomputed. The number of quadrature points  $p$  varies from 30 to 67 among such  $\delta$ .  
 780 This is also the numerical rank for the off-diagonal low-rank approximations. For the  
 781 Gaussian kernel case, they do not depend on  $\delta$  (see Section 2.2.1) because the kernel  
 782 function has no singularity at 0. Accordingly, one set of quadrature nodes and weights  
 783 is sufficient for all Gaussian kernel tests. Note that this set of quadrature nodes and  
 784 weights is calculated from a piece of Matlab code in a double-precision environment.  
 785 This restricts a relative accuracy to up to  $10^{-12}$  for the Gaussian kernel case [21].

786 The tests are performed in Matlab R2021a on a server with two Intel Xeon E5-  
 787 2660V3 CPUs and 192GB of memory.

788 **5.1. Stability of generalized SSS and HSS transforms.** In exact arith-  
 789 metic, the generalized SSS and HSS approximations  $A$  are equal. On the other hand,  
 790 they have different stability behaviors in numerical computations.

791 For the matrix-vector multiplication  $\mathbf{f} = A\mathbf{z}$ , the backward error of an approxi-  
 792 mate product  $\tilde{\mathbf{f}}$  is as follows [18, (3.6)]:

$$793 \quad \varepsilon_{\text{bwd}} = \min\{\varepsilon > 0 : \tilde{\mathbf{f}} = (A + \Delta A)\mathbf{z}, |\Delta A| \leq \varepsilon|A|\} = \max_{i=1:n} \frac{|\tilde{\mathbf{f}}_i - \mathbf{f}_i|}{(|A||\mathbf{z}|)_i},$$

794 where  $\Delta A$  is the perturbation of  $A$  when performing the matrix-vector multiplication.  
 795 This guarantees  $|\Delta A| \leq \varepsilon_{\text{bwd}}|A|$ . According to the stability analysis in Section 4,  
 796 results like (4.7) indicate that a block  $A_{k,l}$  potentially has larger perturbation errors  
 797 when  $|k-l|$  is larger. With fixed finest-level block size  $m$ , in order to test large  $|k-l|$ ,  
 798 large matrix sizes  $n$  are needed. Since it becomes impractical to evaluate  $\mathbf{f}$  via dense  
 799  $A$  when  $n$  is too large, we can just look at the  $m \times m$  finest-level lower-left corner  
 800 block of  $A$  with row index set  $n-m+1:n$  and column index set  $1:m$ . Denote such  
 801 a block by  $A^c$ . We evaluate  $\mathbf{f}^c = A^c\mathbf{z}^c$  with a vector  $\mathbf{z}^c$ . With numerical evaluations  
 802 using either generalized SSS or HSS forms, we obtain  $\tilde{\mathbf{f}}^c = \text{fl}(A^c\mathbf{z}^c)$  and inspect the  
 803 backward error

$$804 \quad (5.1) \quad \varepsilon_{\text{bwd}}^c = \max_{i=1:m} \frac{|\tilde{\mathbf{f}}_i^c - \mathbf{f}_i^c|}{(|A^c||\mathbf{z}^c|)_i}.$$

805 In the stability test, we use  $\mathbf{x}$  with  $n$  equal-spaced data points distributed on  
 806  $[0, 1]$ , where

$$807 \quad n = 2^k \times 10^4, \quad k = 1, 2, \dots, 10.$$

808 Set the size of the corner block  $A^c$  to be  $m = 100$ .  $A^c$  is multiplied with  $\mathbf{z}^c =$   
 809  $(1, \dots, 1)^T$ .

810 With generalized SSS/HSS forms, we plot  $\varepsilon_{\text{bwd}}^c$  in Figure 5.1. For the generalized  
 811 SSS cases,  $\varepsilon_{\text{bwd}}^c$  increases with  $n$  for different kernels. For the generalized HSS cases,  
 812  $\varepsilon_{\text{bwd}}^c$  remains nearly steady for different  $n$ , which aligns with Lemma 4.12. The results  
 813 are consistent with our analysis and confirm the superior stability of transforms via  
 814 generalized HSS structures.

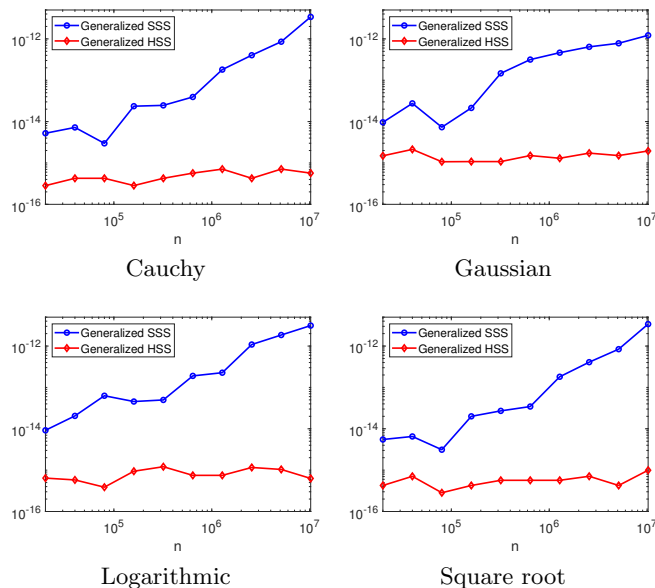


FIG. 5.1. Backward errors  $\varepsilon_{\text{bwd}}^c$  in (5.1), with  $A$  being generalized SSS or HSS approximations to some kernel matrices.

815 **5.2. Efficiency and accuracy of generalized HSS matrix-vector mul-**  
 816 **tiplications.** We now demonstrate the efficiency and accuracy of generalized HSS  
 817 matrix-vector multiplications.  $\mathbf{x}$  has  $n$  random data points uniformly distributed on  
 818  $[0, 1]$ . We set the finest-level block size  $m = 200$ .

819 For Cauchy kernel matrices with varying  $n$ , we report the time to construct the  
 820 generalized HSS approximation from SoE expansions, the time to evaluate matrix-  
 821 vector products with the generators, and the storage for the generators. See Figure 5.2,  
 822 which shows nearly linear complexity and storage. For the other kernels mentioned  
 823 above, the results are similar.

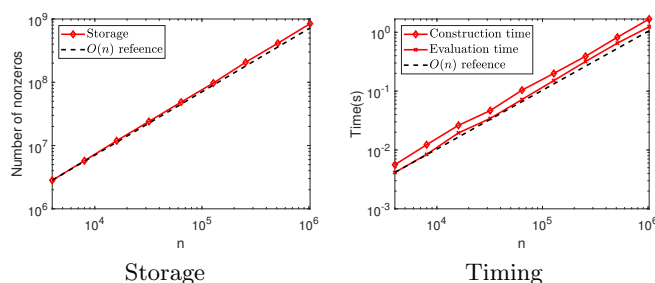


FIG. 5.2. Storage and timing for Cauchy kernel matrices.

824 For the four types of kernel matrices, Table 5.1 shows the relative errors for the  
 825 generalized HSS matrix-vector multiplications. The results confirm the high numerical  
 826 accuracy of the multiplications.

827 **6. Conclusions.** This work reveals how some popular fast transforms via SoE  
 828 expansions are eventually performing certain structured matrix-vector multiplications.  
 829 This in turn leads to a valuable strategy for approximating some kernel matrices via

TABLE 5.1

Relative errors  $\frac{\|A\mathbf{z}-H\mathbf{z}\|_2}{\|H\mathbf{z}\|_2}$  for different kernels and data sizes, where  $H$  is the original kernel matrix.

$n$ ( $\times 10^3$ )	Cauchy	Gaussian	Logarithmic	Square-root
	$\epsilon = 10^{-15}$	$\epsilon = 10^{-12}$	$\epsilon = 10^{-15}$	$\epsilon = 10^{-15}$
4	5.24e-17	2.73e-13	1.34e-15	1.83e-16
8	3.42e-16	3.45e-13	7.25e-16	3.06e-16
16	1.36e-15	3.93e-13	3.68e-15	6.17e-16
32	9.62e-16	4.11e-13	1.53e-14	7.27e-16
64	1.79e-15	4.28e-13	9.66e-15	6.83e-16
128	2.95e-15	4.38e-13	2.18e-15	9.91e-16
256	3.59e-15	4.42e-13	1.95e-14	1.66e-15
512	2.28e-14	4.43e-13	1.83e-14	2.08e-15
1024	5.15e-14	4.43e-13	2.17e-15	3.13e-15

830 SoE expansions. It also gives an intuitive way to study the backward stability of  
831 these transforms. We have shown the stability limitation of the previous transforms  
832 based on generalized SSS forms, and demonstrated how the stability may be further  
833 improved via generalized HSS forms. Following the stability studies, the work even-  
834 tually provides a comprehensive picture of stability issues of structured algorithms.  
835 That is, algorithm architectures and norm bounds of translation generators determine  
836 the backward stability. Hierarchical structured algorithms are typically preferred to  
837 sequential ones. Methods like SoE expansions are nice ways to produce generators  
838 with controlled norms. In future work, it would be interesting to lay out the detailed  
839 matrix structures for algorithms based on higher dimensional SoE expansions like  
840 mentioned in Section 2.3. We expect that the essential ideas of our stability studies  
841 can be naturally extended to higher dimensions.

842

## REFERENCES

- 843 [1] T. BELLA, V. OLSHEVSKY, AND M. STEWART, *Nested product decomposition of quasiseparable*  
844 *matrices*, SIAM J. Matrix Anal. Appl., 34 (2013), pp. 1520–1555.
- 845 [2] G. BEYLKIN AND L. MONZÓN, *On approximation of functions by exponential sums*, Appl. Com-  
846 *put. Harmon. Anal.*, 19 (2005), pp. 17–48.
- 847 [3] G. BEYLKIN, V. CHERUVU, AND F. PÉREZ, *Fast adaptive algorithms in the non-standard form*  
848 *for multidimensional problems*, Appl. Comput. Harmon. Anal., 24 (2008), pp. 354–377.
- 849 [4] G. BEYLKIN, C. KURCZ, AND L. MONZÓN, *Fast algorithms for Helmholtz Green's functions*,  
850 *Proceedings of the Royal Society A: Mathematical, Physical and Engineering Sciences*, 464  
851 (2008), pp. 3301–3326.
- 852 [5] G. BEYLKIN, C. KURCZ, AND L. MONZÓN, *Fast convolution with the free space Helmholtz Green's*  
853 *function*, J. Comput. Phys., 228 (2009), pp. 2770–2791.
- 854 [6] G. BEYLKIN AND L. MONZÓN, *Approximation by exponential sums revisited*, Appl. Comput.  
855 *Harmon. Anal.*, 28 (2010), pp. 131–149.
- 856 [7] J. BREMER, Z. GIMBUTAS, AND V. ROKHLIN, *A nonlinear optimization procedure for generalized*  
857 *Gaussian quadratures*, SIAM J. Sci. Comput., 32 (2010), pp. 1761–1788.
- 858 [8] S. CHANDRASEKARAN AND M. GU, *Fast and stable algorithms for banded plus semiseparable*  
859 *matrices*, SIAM J. Matrix Anal. Appl., 25 (2003), pp. 373–384.
- 860 [9] S. CHANDRASEKARAN, M. GU, AND T. PALS, *A fast ULV decomposition solver for hierarchically*  
861 *semiseparable representations*, SIAM J. Matrix Anal. Appl., 28 (2006), pp. 603–622.
- 862 [10] S. CHANDRASEKARAN, P. DEWILDE, M. GU, T. PALS, X. SUN, A. J. VAN DER VEEN, AND  
863 *D. WHITE, Some fast algorithms for sequentially semiseparable representations*, SIAM J.  
864 *Matrix Anal. Appl.*, 27 (2005), pp. 341–364.
- 865 [11] S. CHANDRASEKARAN, P. DEWILDE, M. GU, T. PALS AND, A. J. VAN DER VEEN, *Fast stable solver*

- 866 for sequentially semi-separable linear systems of equations, in International Conference on  
 867 High-Performance Computing, Springer, Berlin, Heidelberg, 2002, pp. 545–554.
- 868 [12] A. DUTT, M. GU, AND V. ROKHLIN, *Fast algorithms for polynomial interpolation, integration,*  
 869 *and differentiation*, SIAM J. Numer. Anal., 33 (1996), pp. 1689–1711.
- 870 [13] Z. GIMBUTAS, N. F. MARSHALL, AND V. ROKHLIN, *A fast simple algorithm for computing the*  
 871 *potential of charges on a line*, Appl. Comput. Harmon. Anal., 49 (2020), pp. 815–830.
- 872 [14] L. GREENGARD AND V. ROKHLIN, *A fast algorithm for particle simulations*, J. Comput. Phys.,  
 873 73 (1987), pp. 325–348.
- 874 [15] L. GREENGARD AND V. ROKHLIN, *A new version of the fast multipole method for the Laplace*  
 875 *equation in three dimensions*, Acta Numer., 6 (1997), pp. 229–269.
- 876 [16] P. K. GUPTA, S. NIWAS, AND N. CHAUDHARY, *Fast computation of Hankel Transform using*  
 877 *orthonormal exponential approximation of complex kernel function*, J. Earth Syst. Sci., 115  
 878 (2006), pp. 267–276.
- 879 [17] N. J. HIGHAM, *Accuracy and stability of numerical algorithms*, 2nd ed., SIAM, 2002.
- 880 [18] N. J. HIGHAM AND T. MARY, *Sharper probabilistic backward error analysis for basic linear*  
 881 *algebra kernels with random data*, SIAM J. Sci. Comput., 42 (2020), pp. A3427–A3446.
- 882 [19] T. HRYCAK AND V. ROKHLIN, *An improved fast multipole algorithm for potential fields*, SIAM  
 883 J. Sci. Comput., 19 (1998), pp. 1804–1826.
- 884 [20] H. IKENO, *Spherical Bessel transform via exponential sum approximation of spherical Bessel*  
 885 *function*, J. Comput. Phys., 355 (2018), pp. 426–435.
- 886 [21] S. JIANG AND L. GREENGARD, *Approximating the Gaussian as a sum of exponentials and its*  
 887 *applications to the fast gauss transform*, Commun. Comput. Phys., 31 (2022), pp. 1–26.
- 888 [22] P.-D. LÉTOURNEAU, C. CECKA, AND E. DARVE, *Cauchy fast multipole method for general ana-*  
 889 *lytic kernels*, SIAM J. Sci. Comput., 36 (2014), pp. A396–A426.
- 890 [23] P. G. MARTINSSON, *A fast randomized algorithm for computing a hierarchically semiseparable*  
 891 *representation of a matrix*, SIAM J. Matrix Anal. Appl., 32 (2011), pp. 1251–1274.
- 892 [24] X. OU, M. MICHELLE, AND J. XIA, *A stable matrix version of the 2D fast multipole method*,  
 893 SIAM J. Matrix Anal. Appl., 46 (2025), pp. 530–560.
- 894 [25] L. N. TREFETHEN AND M. H. GUTKNECHT, *The Carathéodory–Fejér method for real rational*  
 895 *approximation*, SIAM J. Numer. Anal., 20 (1983), pp. 420–436.
- 896 [26] L. N. TREFETHEN, J. A. C. WEIDEMAN, AND T. SCHMELZER, *Talbot quadratures and rational*  
 897 *approximations*, BIT, 46 (2006), pp. 653–670.
- 898 [27] Y. XI AND J. XIA, *On the stability of some hierarchical rank structured matrix algorithms*,  
 899 SIAM J. Matrix Anal. Appl., 37 (2016), pp. 1279–1303.
- 900 [28] Y. XI, J. XIA, S. CAULEY, AND V. BALAKRISHNAN, *Superfast and stable structured solvers for*  
 901 *Toeplitz least squares via randomized sampling*, SIAM J. Matrix Anal. Appl., 35 (2014), pp.  
 902 44–72.
- 903 [29] J. XIA, S. CHANDRASEKARAN, M. GU, X. S. LI, *Fast algorithms for hierarchically semiseparable*  
 904 *matrices*, Numer. Linear Algebra Appl., 17 (2010), pp. 953–976.
- 905 [30] T. YANAI, G. I. FANN, Z. GAN, R. J. HARRISON, AND G. BEYLKIN, *Multiresolution quantum*  
 906 *chemistry in multiwavelet bases: Hartree-Fock exchange*, J. Chem. Phys., 121 (2004), pp.  
 907 6680–6688.
- 908 [31] N. YARVIN AND V. ROKHLIN, *Generalized Gaussian quadratures and singular value decomposi-*  
 909 *tions of integral operators*, SIAM J. Sci. Comput., 20 (1998), pp. 699–718.
- 910 [32] N. YARVIN AND V. ROKHLIN, *An improved fast multipole algorithm for potential fields on the*  
 911 *line*, SIAM J. Numer. Anal., 36 (1999), pp. 629–666.

912 **A. Appendix: Proofs of the lemmas in Section 4.** This appendix includes  
 913 proofs for some lemmas in the stability analysis. We first give a lemma that will be  
 914 used in later proofs.

915 LEMMA A.1. *Let  $n \in \mathbb{N}_+$  and  $\epsilon$  be a small quantity such that  $0 < n\epsilon < 1/2$ . Then*

$$916 \quad \sum_{k=1}^n \binom{n}{k} \epsilon^k \leq \frac{4}{3} n\epsilon.$$

917 *Proof.* By the binomial theorem, for  $0 < n\epsilon < 1/2$ ,

$$918 \quad \sum_{k=1}^n \binom{n}{k} \epsilon^k \leq \sum_{k=1}^n \frac{(n\epsilon)^k}{k!} \leq (n\epsilon) \sum_{k=0}^{n-1} \left(\frac{n\epsilon}{2}\right)^k \leq \frac{n\epsilon}{1 - (n\epsilon)/2} \leq \frac{4}{3} n\epsilon.$$

919 *Proof of Lemma 4.7.* In the backward traversal stage, we have the following re-  
 920 cursive relation of  $\text{fl}(\mathbf{v}_k)$  through the update formula  $\mathbf{v}_k = Q_k^T \mathbf{z}_k + R_k \mathbf{v}_{k-1}$ :

(A.1)

$$921 \quad \text{fl}(\mathbf{v}_k) = \begin{cases} (I + \Delta Y_1)(Q_1 + \Delta Q_1)^T \mathbf{z}_1, & k = 1, \\ (I + \Delta Y_k) [(Q_k + \Delta Q_k)^T \mathbf{z}_k + (R_k + \Delta R_k) \text{fl}(\mathbf{v}_{k-1})], & 2 \leq k \leq N - 2, \end{cases}$$

922 where  $|\Delta Q_k^T| \leq \tau_m |Q_k^T|$ ,  $|\Delta R_k| \leq \tau_p |R_k|$  by Lemma 4.1, and  $|\Delta Y_k| \leq \epsilon_{\text{mach}} I$ .

923 By expanding the recursive relation (A.1) and applying identity (4.2), we obtain  
 924 the following summation form of  $\text{fl}(\mathbf{v}_k)$ , for  $k = 1, \dots, N - 2$ :

$$925 \quad \text{fl}(\mathbf{v}_k) = \sum_{l=1}^k \left[ \prod_{s=k}^{\geq l+1} (I + \Delta Y_s)(R_s + \Delta R_s) \right] (I + \Delta Y_l)(Q_l + \Delta Q_l)^T \mathbf{z}_l$$

$$926 \quad = \sum_{l=1}^k \left[ \prod_{s=k}^{\geq l+1} R_s + \sum_{|\xi|=1}^{k-l} \Delta^\xi \left( \prod_{s=k}^{\geq l+1} \tilde{R}_s \right) \right] (Q_l + \Delta \tilde{Q}_l)^T \mathbf{z}_l$$

$$927 \quad =: \mathbf{v}_k + \Delta \mathbf{v}_k \quad \text{with}$$

$$928 \quad \Delta \mathbf{v}_k = \sum_{l=1}^k \left[ \sum_{|\xi|=1}^{k-l+1} \Delta^\xi \left[ \left( \prod_{s=k}^{\geq l+1} \tilde{R}_s \right) \tilde{Q}_l^T \right] \right] \mathbf{z}_l,$$

929 where  $\Delta^\xi \tilde{Q}_l^T$  and  $\Delta^\xi \tilde{R}_s$ , for  $\xi \in \{0, 1\}$ , are given by (4.5) and (4.6), respectively.

930 With Assumption 4.5,  $Q_l^T$  is a  $p \times m$  matrix for each  $l$ . Then,  $\|Q_l^T\|_1 \leq c_U p$ .

931 Thus, with (4.5) and (4.6),

$$932 \quad \|\Delta^1 \tilde{Q}_l^T\|_1 \leq \tau_m \|Q_l^T\|_1 + \epsilon_{\text{mach}} \|Q_l^T\|_1 + \epsilon_{\text{mach}} \tau_p \|Q_l^T\|_1 \leq p c_U \tau_{3m},$$

$$933 \quad \|\Delta^1 \tilde{R}_s\|_1 \leq \tau_p \|R_s\|_1 + \epsilon_{\text{mach}} \|R_s\|_1 + \epsilon_{\text{mach}} \tau_p \|R_s\|_1 \leq c_T \tau_{3p}. \quad \square$$

934 *Proof of Lemma 4.8.* In this stage, we compute  $\text{fl}(\mathbf{f}_k^+)$  by multiplying  $P_k B$  with  
 935  $\text{fl}(\mathbf{v}_{k-2})$  defined in (4.4). Combing with the definition of  $\Delta \mathbf{v}_{k-2}$  in Lemma 4.7 to get

$$936 \quad \text{fl}(\mathbf{f}_k^+) = (P_k + \Delta P_k)(B + \Delta B) \text{fl}(\mathbf{v}_{k-2}) = P_k B \mathbf{v}_{k-2} + \sum_{|\xi|=1}^3 \Delta^\xi (P_k B \mathbf{v}_{k-2})$$

$$937 \quad = \mathbf{f}_k^+ + \Delta \mathbf{f}_k^+ \quad \text{with}$$

$$938 \quad (A.2) \quad \Delta \mathbf{f}_k^+ = \sum_{l=1}^{k-2} \left[ \sum_{|\xi|=1}^{k-l+1} \Delta^\xi \left[ P_k B \left( \prod_{s=k-2}^{\geq l+1} \tilde{R}_s \right) \tilde{Q}_l^T \right] \right] \mathbf{z}_l,$$

939 where  $|\Delta B| \leq \tau_p |B|$ ,  $|\Delta P_k| \leq \tau_p |P_k|$  by Lemma 4.1 and  $\Delta^\xi \tilde{Q}_l^T$  and  $\Delta^\xi \tilde{R}_s$  are respec-  
 940 tively defined as in (4.5) and (4.6).

941 Let  $\Delta \tilde{A}_{k,l} := \sum_{|\xi|=1}^{k-l+1} \Delta^\xi \left[ P_k B \left( \prod_{s=k-2}^{\geq l+1} \tilde{R}_s \right) \tilde{Q}_l^T \right]$  for  $k > l + 1$ . It has the fol-  
 942 lowing norm relation by setting  $\xi = (\xi_k, \xi_{k-1}, \dots, \xi_l)$  and using Lemma 4.3:

$$943 \quad (A.3) \quad \|\Delta \tilde{A}_{k,l}\|_{\max} \leq \sum_{|\xi|=1}^{k-l+1} \|\Delta^{\xi_k} P_k\|_{\infty} \|\Delta^{\xi_{k-1}} B\|_{\max} \prod_{s=k-2}^{\geq l+1} \|\Delta^{\xi_s} \tilde{R}_s\|_1 \|\Delta^{\xi_l} \tilde{Q}_l^T\|_1.$$

944 To bound the right-hand side of (A.3), we list the norm bounds for the matrices  
 945 (derived from Assumption 4.5 or given in Lemma 4.7):

$$\begin{aligned}
 946 \quad & \|\Delta^0 P_k\|_\infty \leq p c_U, \quad \|\Delta^0 B\|_{\max} \leq c_B |A|_{\min}, \quad \|\Delta^0 \tilde{R}_s\|_1 \leq c_T, \quad \|\Delta^0 \tilde{Q}_l^T\|_1 \leq p c_U, \\
 947 \quad & \|\Delta^1 P_k\|_\infty \leq p c_U \tau_p, \quad \|\Delta^1 B\|_{\max} \leq c_B \tau_p |A|_{\min}, \quad \|\Delta^1 \tilde{R}_s\|_1 \leq c_T \tau_{3p}, \\
 948 \quad & \|\Delta^1 \tilde{Q}_l^T\|_1 \leq p c_U \tau_{3m}.
 \end{aligned}$$

949 Thus, from (A.3) and Lemma A.1, we obtain

$$\begin{aligned}
 950 \quad |\Delta \tilde{A}_{k,l}| & \leq \|\Delta \tilde{A}_{k,l}\|_{\max} \leq \sum_{|\xi|=1}^{k-l+1} (p c_U \tau_p^{|\xi|}) (c_B |A|_{\min} \tau_p^{|\xi|-1}) \left( \prod_{s=k-2}^{\geq l+1} c_T \tau_{3p}^{|\xi_s|} \right) (p c_U \tau_{3m}^{|\xi|}) \\
 951 \quad & \leq \sum_{|\xi|=1}^{k-l+1} \binom{k-l+1}{|\xi|} p^2 c_B c_U^2 c_T^{k-l-2} |A|_{\min} \tau_{3m}^{|\xi|} \\
 952 \quad & \leq \frac{4}{3} (k-l+1) \tau_{3m} p^2 c_B c_U^2 c_T^{k-l-2} |A_{k,l}|. \quad \square
 \end{aligned}$$

953 *Proof of Lemma 4.11.* Following the bottom-up traversal in (3.10), we obtain the  
 954 following equation for  $1 \leq i \leq L$  via the recursive relations by noting  $\mathbf{z}^{(L+1)} = \hat{\mathbf{z}}$ :

$$955 \quad \mathfrak{fl}(\mathbf{z}^{(i)}) = \prod_{j=i}^L (V^{(j)} + \Delta V^{(j)})^T \mathbf{z}^{(L+1)} = \left( \prod_{j=i}^L (V^{(j)})^T + \sum_{|\xi|=1}^{L-i+1} \Delta^\xi \prod_{j=i}^L (V^{(j)})^T \right) \mathbf{z}^{(L+1)},$$

956 where

$$957 \quad (\text{A.4}) \quad |(\Delta V^{(j)})^T| \leq \begin{cases} \tau_m |(V^{(j)})^T|, & \text{if } j = L, \\ \tau_{2p} |(V^{(j)})^T|, & \text{if } 1 \leq j < L, \end{cases}$$

958 by Lemma 4.1. Hence,  $|(\Delta V^{(j)})^T| \leq \tau |(V^{(j)})^T|$ , with  $\tau = \max\{\tau_m, \tau_{2p}\}$ , for all  $j$ .

959 The coefficient for the case  $j = L$  in (A.4) is  $\tau_m$  because  $(V^{(L)})^T$  is a block  
 960 diagonal matrix with the blocks  $\{\mathcal{V}_i^T\}$  defined in (3.9) and each  $\mathcal{V}_i^T$  is a  $p \times m$  matrix  
 961 by Assumption 4.5. Based on this, we also obtain

$$962 \quad \|(V^{(L)})^T\|_1 \leq p c_U \quad \text{and} \quad \|(\Delta V^{(L)})^T\|_1 \leq p c_U \tau_m.$$

963 For the cases when  $1 \leq j < L$  in (A.4), the coefficient would be  $\tau_{2p}$  since  $(V^{(j)})^T$  is a  
 964 block diagonal matrix with  $p \times 2p$  blocks  $(\mathcal{W}_{c_1}^T \quad \mathcal{W}_{c_2}^T)$ . Accordingly, for  $1 \leq j < L$ ,

$$965 \quad \|(V^{(j)})^T\|_1 \leq c_T \quad \text{and} \quad \|(\Delta V^{(j)})^T\|_1 \leq c_T \tau_{2p}.$$

966 Thus, by Assumption 4.5, for  $1 \leq i \leq L$ ,

$$967 \quad \left\| \Delta^\xi \prod_{j=i}^L (V^{(j)})^T \right\|_1 \leq \tau_{2m}^{|\xi|} \prod_{j=i}^L \|(V^{(j)})^T\|_1 \leq p c_U c_T^{L-i} \tau_{2m}^{|\xi|}.$$

968 For  $\mathfrak{fl}(\mathbf{y}^{(i)})$  obtained via recursive formulae in (3.10), we have

$$\begin{aligned}
 969 \quad \mathfrak{fl}(\mathbf{y}^{(i)}) & = (B^{(i)} + \Delta B^{(i)}) \left( \prod_{j=i}^L (V^{(j)})^T + \sum_{|\xi|=1}^{L-i+1} \Delta^\xi \prod_{j=i}^L (V^{(j)})^T \right) \mathbf{z}^{(L+1)} \\
 970 \quad & = \mathbf{y}^{(i)} + \left( \sum_{|\xi|=1}^{L-i+2} \Delta^\xi \left( B^{(i)} \prod_{j=i}^L (V^{(j)})^T \right) \right) \mathbf{z}^{(L+1)},
 \end{aligned}$$

971 with  $|\Delta B^{(i)}| \leq \tau_p |B^{(i)}|$  for  $1 \leq i \leq L$ .  $\square$

972 *Proof of Lemma 4.12.* Following the top-down traversal in (3.11), the following  
973 expansion of  $\text{fl}(\mathbf{f}^{(i)})$  holds for  $1 \leq i \leq L-1$ :

$$\begin{aligned} 974 \quad \text{fl}(\mathbf{f}^{(i)}) &= (I + \Delta Z^{(i)})(U^{(i)} + \Delta U^{(i)}) \text{fl}(\mathbf{f}^{(i-1)}) + \text{fl}(\mathbf{y}^{(i+1)}) \\ 975 &= \sum_{k=1}^{i+1} (I + \Delta Z^{(i)}) \left( \prod_{j=i}^{\geq k} [(U^{(j)} + \Delta U^{(j)})(I + \Delta Z^{(j-1)})] \right) \text{fl}(\mathbf{y}^{(k)}), \end{aligned}$$

976 where  $|\Delta Z^{(j)}| \leq \epsilon_{\text{mach}} I$ , and  $\Delta U^{(j)}$  is a block diagonal matrix with block size  $2p \times p$   
977 that satisfies  $|\Delta U^{(j)}| \leq \tau_p |U^{(j)}|$  according to Lemma 4.1. Hence, for  $1 \leq j \leq L-1$ ,

$$978 \quad (\text{A.5}) \quad \|U^{(j)}\|_{\infty} \leq c_T, \quad \|\Delta U^{(j)}\|_{\infty} \leq c_T \tau_p.$$

979 By multiplying  $U^{(L)}$  with  $\text{fl}(\mathbf{f}^{(L-1)})$  in the evaluation stage, we have

$$\begin{aligned} 980 \quad (\text{A.6}) \quad \text{fl}(\hat{A}_{\mathbf{L}} \mathbf{z}^{(L+1)}) &= (U^{(L)} + \Delta U^{(L)}) \text{fl}(\mathbf{f}^{(L-1)}) \\ 981 &= \sum_{k=1}^L \left( \prod_{j=L}^{\geq k} [(U^{(j)} + \Delta U^{(j)})(I + \Delta Z^{(j-1)})] \right) \text{fl}(\mathbf{y}^{(k)}) \\ 982 &= \sum_{k=1}^L \left( \prod_{j=L}^{\geq k} U^{(j)} + \sum_{|\xi|=1}^{L-k+1} \Delta^{\xi} \left( \prod_{j=L}^{\geq k} \tilde{U}^{(j)} \right) \right) \text{fl}(\mathbf{y}^{(k)}), \end{aligned}$$

983 where

$$984 \quad \Delta^0 \tilde{U}^{(j)} = U^{(j)}, \quad \Delta^1 \tilde{U}^{(j)} = \Delta U^{(j)} + U^{(j)} \Delta Z^{(j-1)} + \Delta U^{(j)} \Delta Z^{(j-1)},$$

985 and  $\Delta U^{(L)}$  is a block diagonal matrix with block size  $m \times p$  that satisfies  $|\Delta U^{(L)}| \leq$   
986  $\tau_p |U^{(L)}|$ . Thus,

$$987 \quad (\text{A.7}) \quad \|\Delta \tilde{U}^{(j)}\|_{\infty} \leq (\tau_p + \epsilon_{\text{mach}} + \epsilon_{\text{mach}} \tau_p) \|U^{(j)}\|_{\infty} \leq \tau_{3p} \|U^{(j)}\|_{\infty} \leq c_T \tau_{3p},$$

988 and by Assumption 4.5,

$$989 \quad (\text{A.8}) \quad \|U^{(L)}\|_{\infty} \leq pc_U \quad \text{and} \quad \|\Delta U^{(L)}\|_{\infty} \leq pc_U \tau_p.$$

990 Moreover, if we combine (A.5), (A.8) together with (A.7), we get

$$991 \quad (\text{A.9}) \quad \left\| \Delta^{\xi} \prod_{j=L}^{\geq k} \tilde{U}^{(j)} \right\|_{\infty} \leq \tau_{3p}^{|\xi|} \prod_{j=L}^{\geq k} \|\tilde{U}^{(j)}\|_{\infty} \leq pc_U c_T^{L-k} \tau_{3p}^{|\xi|}, \quad \text{for } 1 \leq k \leq L.$$

992 Next, we discuss the perturbation  $\Delta \hat{A}_{\mathbf{L}}$ . If we plug (4.14) into (A.6), we obtain  
993  $\text{fl}(\hat{A}_{\mathbf{L}} \mathbf{z}^{(L+1)}) = \hat{A}_{\mathbf{L}} \mathbf{z}^{(L+1)} + \Delta \hat{A}_{\mathbf{L}} \mathbf{z}^{(L+1)}$  with  $\Delta \hat{A}_{\mathbf{L}}$  defined in (4.15). To analyze  $|\Delta \hat{A}_{\mathbf{L}}|$ ,  
994 we observe that the nonzero patterns of  $\Delta \hat{A}_{\mathbf{L}}^{(k)}$  defined in (4.16) do not overlap for  
995 distinct  $k$ . Then

$$996 \quad (\text{A.10}) \quad |\Delta \hat{A}_{\mathbf{L}}| \leq \|\Delta \hat{A}_{\mathbf{L}}\|_{\max} \leq \max_{1 \leq k \leq L} \|\Delta \hat{A}_{\mathbf{L}}^{(k)}\|_{\max}.$$

997 Hence, it suffices to find an upper bound for  $\|\Delta\hat{A}_{\mathbf{L}}^{(k)}\|_{\max}$ , for each  $k$ .

998 Let  $\boldsymbol{\xi} = (\boldsymbol{\xi}_1, \boldsymbol{\xi}_2, \boldsymbol{\xi}_3)$ . Based on (4.16), we use norm bounds (A.9) and Lemma 4.11  
999 to obtain

$$\begin{aligned}
1000 \quad \|\Delta\hat{A}_{\mathbf{L}}^{(k)}\|_{\max} &\leq \sum_{|\boldsymbol{\xi}|=1}^{2L-2k+3} \left\| \Delta^{\boldsymbol{\xi}_1} \prod_{j=L}^{\geq k} \tilde{U}^{(j)} \right\|_{\infty} \left\| \Delta^{\boldsymbol{\xi}_2} B^{(k)} \right\|_{\max} \left\| \Delta^{\boldsymbol{\xi}_3} \prod_{j=k}^L (V^{(j)})^T \right\|_1 \\
1001 \quad &\leq \sum_{|\boldsymbol{\xi}|=1}^{2L-2k+3} p c_U c_T^{L-k} \tau_{3p}^{|\boldsymbol{\xi}_1|} c_B |A|_{\min} \tau_p^{|\boldsymbol{\xi}_2|} p c_U c_T^{L-k} \tau_{2m}^{|\boldsymbol{\xi}_3|} \\
1002 \quad &\leq p^2 c_B c_U^2 c_T^{2L-2k} |A|_{\min} \sum_{|\boldsymbol{\xi}|=1}^{2L-2k+3} \binom{2L-2k+3}{|\boldsymbol{\xi}|} \tau_{3m}^{|\boldsymbol{\xi}|} \\
1003 \quad &\leq \frac{4}{3} (2L-2k+3) p^2 c_B c_U^2 c_T^{2L-2k} \tau_{3m} |\hat{A}_{\mathbf{L}}|,
\end{aligned}$$

1004 where the last step is given by Lemma A.1.

1005 By applying (A.10) and Assumption 4.5, we obtain (4.17). □